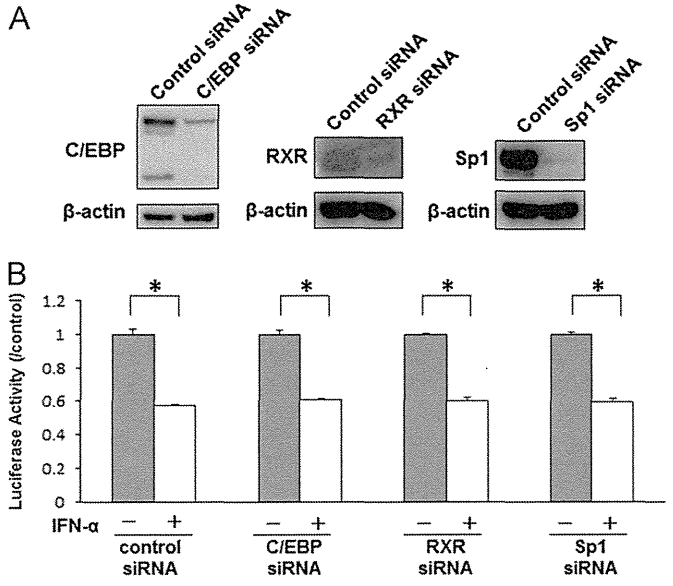

Fig. 6. IFN-α-mediated suppression on En II activity with knockdown of C/EBP, RXR and Sp1. A. Huh-7 cells were transfected with 10 nM siRNA (negative control or specific for C/EBP, RXR and Sp1). Immunoblot analyses for expressions of C/EBP, RXR, Sp1 and β-actin were performed at 48 h post siRNA transfection. B. Huh-7 cells were transfected with 10 nM siRNA (negative control or specific for C/EBP, RXR and Sp1). On the next day, si-RNA treated cells were transfected again with pGL4LUC-En II. On the following day, these transfected cells were incubated with IFN-α(1000 IU/ml) for 12 h, and luciferase activities were evaluated. "/control" on the vertical axis means the ratio of luciferase activity of IFN-α treated cells normalized with that of non-treated cells.

pan-PKC inhibitor sotrastaurin did not affect HBV replication. While the role of PKC in the HBV life cycle is still controversial, our findings suggest that PKC isoforms activated by IFN-α play inhibitory roles in HBV transcription by down-regulation of En II activity. As von Hahn et al. reported, sotrastaurin alone did not affect HBV replication. But, based on our present data about another pan-PKC inhibitor, staurosporine, we speculate that sotrastaurin may also block the inhibitory effect of IFN-α on En II activity.

We showed that knockdown of a single transcription factor did not influence the IFN-α-mediated suppression of En II activity, suggesting that several transcription factors might be involved in this suppression. We also showed that both segment 4 (nt 1703–1727) and segment 6 (nt 1746–1770) within the En II region are required for the IFN-α-induced suppression of En II activity. Although these two regions seem to be more important than the others, all the deleted version of reporter constructs showed almost completely similar suppression activities (Fig. 3B). We speculate that there may be some transcription factors which affect both the segment 4 and 6. Even if one of these regions is deleted, some factors may affect the other region, and result in the suppression of En II activity. Further study will be needed to clarify the mechanism.

Indeed, there are no identified transcription factors which could bind both segment 4 and 6. Only two transcription factors (HNF1 and 3) were reported to bind segment 4 (Johnson et al., 1995; Wang et al., 1998), and there have been no reports indicating that IFN-α or PKC inactivates HNF1 or 3. We also examined the expression levels of HNF1 and 3 of the IFN-α treated and the non-treated cells by RT-PCR. There was no significant difference in the expression of these transcription factors between the IFN-α treated and the non-treated cells (Nawa et al., unpublished data). Thus, we speculate that HNF1 or 3 might not be involved in the IFN-α mediated suppression of En II activity. There may be unknown transcription factors in the PKC pathway.

Previous reports showed that IFN-α suppressed En I activity (Nakao et al., 1999; Tur-Kaspa et al., 1990). Nakao et al. (1999) indicated that this occurred due to the binding of ISGF3 to an ISRE-like motif within the En I region. However, Rang et al. (2001) demonstrated that IFN-α reduced HBV-RNA levels derived from both HBV genome wild type and mutated ISRE-like motifs. This result contradicted the Nakao's result that the activity of the En I mutated ISRE-like motif was not suppressed by IFN-α. Schulte-Frohlinde et al. (2002) reported that IFN-α suppressed HBV core promoter regulated transcriptional activity, even when the ISRE-like motif of En I was deleted. The results of Rang et al. and Schulte-Frohlinde et al. suggest that IFN-α might suppress the activity of regions other than En I. In the present study, we demonstrated that IFN-α suppressed En II activity via the PKC pathway. En II might be one of the candidate regions down-regulated by IFN-α within the HBV genome.

Since En II activates viral transcription only in hepatocytes, it is responsible for the hepatocyte-specific gene expression of HBV. There had been no study on the effect of IFN-α on En II activity. Our study clarified that the PKC pathway is involved in the IFN-α-mediated suppression of En II activity, but may not involve ISG induction. Our result should aid in establishing better treatment with IFN-α against HBV infection. As we could not determine the molecule which inhibits En II activity by IFN-α, further study is needed to clarify this molecule and to control hepatitis B by IFN-α treatment.

Materials and methods

Plasmids

The HBV sequence used in this study was of the *adw2* subtype (GenBank accession no. X02763). Numbering of the HBV sequence started at the unique *EcoRI* site. The En II region in this study was defined as nt 1640–1771 of HBV sequence (Fig. 1) (Ishida et al., 2000). To construct pGL4LUC-En II, a plasmid containing the HBV En II region, the DNA fragment was amplified with PCR and inserted between *Hind* III and *Nhe* I site of pGL4 Luciferase Reporter Vector (pGL4LUC) (Promega, Madison, WI). The PCR primers were as follows: 5′-CCAAGCTTCTGCCCAAGGTC-3′ and 5′-CCCGCTAGCAAAGACCTTTAACCTAATCTCCTCC-3′. The constructs of the En II sequence with various deletions were generated by modifying pGL4LUC-En II using the QuikChange Site-Directed Mutagenesis Kit (Stratagene, La Jolla, CA). The constructs containing four tandem repeats of short fragment in En II sequence were generated by inserting duplexes of synthesized oligonucleotides into the multi-cloning site of pGL4LUC. All of the En II sequences were inserted in the antisense orientation to evaluate their enhancer activity.

Plasmid pHBV1.5 containing a 1.5-fold-overlength genome of HBV-DNA (GenBank accession no. AF305422) has been described previously (Bruss and Ganem, 1991).

Cell lines and reagents

The human hepatocellular carcinoma cell lines Huh-7, PLC/PRF/5, and Hep3B were cultured in Dulbecco's modified Eagle's medium (DMEM) supplemented with 10% heat-inactivated fetal bovine serum (Sigma-Aldrich, St. Louis, MO) in a humidified incubator at 5% CO_2 and 37 °C. Human natural IFN-α was kindly provided by Hayashibara Biochemical Laboratories, Inc. (Okayama, Japan).

The inhibitors/activators and the final concentrations used were: JAK inhibitor I (1 μM), PD98059 (10 μM), SB203580 (10 μM), LY294002 (10 μM), Akt-I-1/2 (5 μM), staurosporine (10 or 20 nM), rottlerin (5 μM), Gö6976 (1 μM), SP600125 (10 μM)

(Calbiochem, San Diego, CA), phorbol 12-myristate 13-acetate (PMA) (100 nM) (Sigma-Aldrich, St. Louis, MO).

Plasmid transfection and luciferase assay

Huh-7 cells were co-transfected with the firefly luciferase plasmid and pGL4-RL-tk, an expression vector of renilla luciferase, which was used as an internal control, using FuGENE HD reagent (Roche Applied Science, Indianapolis, IN) according to the manufacturer's protocol. Activities of firefly luciferase and renilla luciferase were measured using the Dual-Glo Luciferase Assay System (Promega, Madison, WI), and then relative luciferase activity was calculated by normalizing firefly luciferase activity to renilla luciferase activity.

RNA extraction

Total RNA was isolated from cells using ISOGEN (Nippon Gene, Tokyo, Japan) according to the manufacturer's protocol. The isolated RNA was treated with DNase I (Promega, Madison, WI) to avoid contamination with transfected plasmid, and then purified with a mixture of phenol, chloroform, and isoamylalcohol (pH 7.9), followed by ethanol precipitation.

Western blot analysis

Cultured cells were lysed with a lysis buffer (1% NP-40, 0.5% sodium deoxycholate, 0.1% SDS, and protein inhibitor cocktail (Nacalai Tesque), in PBS, pH 7.4). Equal amounts of protein were electrophoretically separated by polyacrylamide gel and transferred onto PVDF membrane. For immunodetection, the following antibodies were used: anti-STAT1 antibody, anti-phospho-STAT1 antibody, anti-phospho-PKC-α/β II (Thr 638/641) antibody, anti-phospho-PKC-δ (Thr 505) antibody, anti-C/EBP antibody, anti-RXR antibody, anti-Sp1 antibody, anti-β-actin antibody from Cell Signaling Technology (Beverly, MA), and anti-Mx antibody from Abcam (Cambridge, UK). The signals of phosphorylated proteins such as phospho-PKC-α/β, -δ and phospho-STAT1 were analyzed quantitatively using image analyzing software (ImageJ; version 1.45).

Small RNA interference

Stealth Select RNAi specific for STAT1 (HSS 10273) was purchased from Invitrogen (Carlsbad, CA). Silencer Select siRNA specific for C/EBP (ID: S2890), RXR (ID: S12386) and Sp1 (ID: S13319) were purchased from Ambion (Austin, TX). Stealth RNAi Negative Control Low GC Duplex (Invitrogen, Carlsbad, CA) was used as a control for the off-target effect following Stealth Select RNAi delivery. The transfections were carried out using Lipofectamine RNAiMAX (Invitrogen, Carlsbad, CA) according to the reverse transfection protocol.

Real-time reverse-transcription PCR

For cDNA synthesis, 1 μg of total RNA was reverse-transcribed using High Capacity RNA-to-DNA Master Mix (Applied Biosystems, Foster City, CA). cDNA, equivalent to 20 ng RNA, was used as a template for real-time reverse-transcription PCR (RT-PCR) using Applied Biosystems 7900HT Fast Real-Time PCR System (Applied Biosystems, Foster City, CA). mRNA expressions of C/EBP, FTF, HNF1, HNF3, and HNF4 were measured using TaqMan Gene Expression Assays and were corrected with the quantified expressions level of β-actin mRNA. Assay IDs for the genes were as follows: C/EBP (Hs00269972_s1), FTF (Hs00187067_m1), HNF1 (Hs00167041_m1), HNF3 (Hs00232754_m1), and HNF4 (Hs01023298_m1).

For the detection of pgRNA and pre-C mRNA, the primers and the probes were designed as follows according to a previous study (Laras et al., 2002): the sense primer was 5′-TCTTGTACATGTCCCACTGTTCAA-3′ (nt 1843–1866); the anti-sense primer was 5′-AATGCCATGCCCCAAAGC-3′ (nt 1890–1909); the probe was 5′-FAM-CTCCAAGCTGTGCCTT -3′ (nt 1869–1884). Since they were within precore/core coding sequence, only the total abundance of pgRNA and pre-C RNA could be detected.

Statistical analysis

Data were presented as mean ± SD. Differences between two groups were determined using Student's t-test for unpaired observations. $p < 0.05$ was considered statistically significant.

Disclosures

All authors have nothing to disclose.

References

Antonucci, T.K., Rutter, W.J., 1989. Hepatitis B virus (HBV) promoters are regulated by the HBV enhancer in a tissue-specific manner. J. Virol. 63, 579–583.
Azzi, A., Boscoboinik, D., Hensey, C., 1992. The protein kinase C family. Eur. J. Biochem. 208, 547–557.
Beck, J., Nassal, M., 2007. Hepatitis B virus replication. World J. Gastroenterol. 13, 48–64.
Breitkreutz, D., Braiman-Wiksman, L., Daum, N., Denning, M.F., Tennenbaum, T., 2007. Protein kinase C family: on the crossroads of cell signaling in skin and tumor epithelium. J. Cancer Res. Clin. Oncol. 133, 793–808.
Bruss, V., Ganem, D., 1991. The role of envelope proteins in hepatitis B virus assembly. Proc. Nat. Acad. Sci. U.S.A. 88, 1059–1063.
Caraglia, M., Abbruzzese, A., Leardi, A., Pepe, S., Budillon, A., Baldassare, G., Selleri, C., Lorenzo, S.D., Fabbrocini, A., Giuberti, G., Vitale, G., Lupoli, G., Bianco, A.R., Tagliaferri, P., 1999. Interferon-alpha induces apoptosis in human KB cells through a stress-dependent mitogen activated protein kinase pathway that is antagonized by epidermal growth factor. Cell Death Differ. 6, 773–780.
Castagna, M., Takai, Y., Kaibuchi, K., Sano, K., Kikkawa, U., Nishizuka, Y., 1982. Direct activation of calcium-activated, phospholipid-dependent protein kinase by tumor-promoting phorbol esters. J. Biol. Chem. 257, 7847–7851.
Darnell, J.E., Kerr, I.M., Stark, G.R., 1994. Jak-STAT pathways and transcriptional activation in response to IFNs and other extracellular signaling proteins. Science 264, 1415–1421.
David, M., Petricoin, E., Benjamin, C., Pine, R., Weber, M.J., Larner, A.C., 1995. Requirement for MAP kinase (ERK2) activity in interferon alpha- and interferon beta-stimulated gene expression through STAT proteins. Science 269, 1721–1723.
Delmotte, M.H., Tahayato, A., Formstecher, P., Lefebvre, P., 1999. Serine 157, a retinoic acid receptor alpha residue phosphorylated by protein kinase C in vitro, is involved in RXR.RARalpha heterodimerization and transcriptional activity. J. Biol. Chem. 274, 38225–38231.
Der, S.D., Zhou, A., Williams, B.R., Silverman, R.H., 1998. Identification of genes differentially regulated by interferon alpha, beta, or gamma using oligonucleotide arrays. Proc. Nat. Acad. Sci. U.S.A. 95, 15623–15628.
Goh, K.C., Haque, S.J., Williams, B.R., 1999. p38 MAP kinase is required for STAT1 serine phosphorylation and transcriptional activation induced by interferons. EMBO J. 18, 5601–5608.
Griner, E.M., Kazanietz, M.G., 2007. Protein kinase C and other diacylglycerol effectors in cancer. Nat. Rev. Cancer 7, 281–294.
Gschwendt, M., Müller, H.J., Kielbassa, K., Zang, R., Kittstein, W., Rincke, G., Marks, F., 1994. Rottlerin, a novel protein kinase inhibitor. Biochem. Biophys. Res. Commun. 199, 93–98.
Guo, W., Chen, M., Yen, T.S., Ou, J.H., 1993. Hepatocyte-specific expression of the hepatitis B virus core promoter depends on both positive and negative regulation. Mol. Cell. Biol. 13, 443–448.
Ishida, H., Ueda, K., Ohkawa, K., Kanazawa, Y., Hosui, A., Nakanishi, F., Mita, E., Kasahara, A., Sasaki, Y., Hori, M., Hayashi, N., 2000. Identification of multiple transcription factors, HLF, FTF, and E4BP4, controlling hepatitis B virus enhancer II. J. Virol. 74, 1241–1251.
Johnson, J.L., Raney, A.K., McLachlan, A., 1995. Characterization of a functional hepatocyte nuclear factor 3 binding site in the hepatitis B virus nucleocapsid promoter. Virology 208, 147–158.
Jonas, M.M., Block, J.M., Haber, B.A., Karpen, S.J., London, W.T., Murray, K.F., Narkewicz, M.R., Rosenthal, P., Schwarz, K.B., McMahon, B.J., Foundation, H.B., 2010. Treatment of children with chronic hepatitis B virus infection in the United States: patient selection and therapeutic options. Hepatology 52, 2192–2205.

Kang, H., Yu, J., Jung, G., 2008. Phosphorylation of hepatitis B virus core C-terminally truncated protein (Cp149) by PKC increases capsid assembly and stability. Biochem. J. 416, 47–54.
Kaur, S., Parmar, S., Smith, J., Katsoulidis, E., Li, Y., Sassano, A., Majchrzak, B., Uddin, S., Tallman, M.S., Fish, E.N., Platanias, L.C., 2005. Role of protein kinase C-delta (PKC-delta) in the generation of the effects of IFN-alpha in chronic myelogenous leukemia cells. Exp. Hematol. 33, 550–557.
Kikkawa, U., Kishimoto, A., Nishizuka, Y., 1989. The protein kinase C family: heterogeneity and its implications. Annu. Rev. Biochem. 58, 31–44.
Laras, A., Koskinas, J., Hadziyannis, S.J., 2002. In vivo suppression of precore mRNA synthesis is associated with mutations in the hepatitis B virus core promoter. Virology 295, 86–96.
Li, M., Xie, Y., Wu, X., Kong, Y., Wang, Y., 1995. HNF3 binds and activates the second enhancer, ENII, of hepatitis B virus. Virology 214, 371–378.
Li, M., Xie, Y.H., Kong, Y.Y., Wu, X., Zhu, L., Wang, Y., 1998. Cloning and characterization of a novel human hepatocyte transcription factor, hB1F, which binds and activates enhancer II of hepatitis B virus. J. Biol. Chem. 273, 29022–29031.
Liaw, Y.F., 2009. HBeAg seroconversion as an important end point in the treatment of chronic hepatitis B. Hepatol. Int.
Lok, A.S., McMahon, B.J., 2009. Chronic hepatitis B: update 2009. Hepatology 50, 661–662.
López-Cabrera, M., Letovsky, J., Hu, K.Q., Siddiqui, A., 1990. Multiple liver-specific factors bind to the hepatitis B virus core/pregenomic promoter: trans-activation and repression by CCAAT/enhancer binding protein. Proc. Nat. Acad. Sci. U.S.A. 87, 5069–5073.
López-Cabrera, M., Letovsky, J., Hu, K.Q., Siddiqui, A., 1991. Transcriptional factor C/EBP binds to and transactivates the enhancer element II of the hepatitis B virus. Virology 183, 825–829.
Mahoney, C.W., Shuman, J., McKnight, S.L., Chen, H.C., Huang, K.P., 1992. Phosphorylation of CCAAT-enhancer binding protein by protein kinase C attenuates site-selective DNA binding. J. Biol. Chem. 267, 19396–19403.
Marte, B.M., Meyer, T., Stabel, S., Standke, G.J., Jaken, S., Fabbro, D., Hynes, N.E., 1994. Protein kinase C and mammary cell differentiation: involvement of protein kinase C alpha in the induction of beta-casein expression. Cell Growth Differ. 5, 239–247.
Martiny-Baron, G., Kazanietz, M.G., Mischak, H., Blumberg, P.M., Kochs, G., Hug, H., Marmé, D., Schächtele, C., 1993. Selective inhibition of protein kinase C isozymes by the indolocarbazole Gö 6976. J. Biol. Chem. 268, 9194–9197.
Moolla, N., Kew, M., Arbuthnot, P., 2002. Regulatory elements of hepatitis B virus transcription. J. Viral. Hepat. 9, 323–331.
Nakao, K., Nakata, K., Yamashita, M., Tamada, Y., Hamasaki, K., Ishikawa, H., Kato, Y., Eguchi, K., Ishii, N., 1999. p48 (ISGF-3gamma) is involved in interferon-alpha-induced suppression of hepatitis B virus enhancer-1 activity. J. Biol. Chem. 274, 28075–28078.
Nishizuka, Y., 1988. The molecular heterogeneity of protein kinase C and its implications for cellular regulation. Nature 334, 661–665.
Pal, S., Claffey, K.P., Cohen, H.T., Mukhopadhyay, D., 1998. Activation of Sp1-mediated vascular permeability factor/vascular endothelial growth factor transcription requires specific interaction with protein kinase C zeta. J. Biol. Chem. 273, 26277–26280.
Pfeffer, L.M., Eisenkraft, B.L., Reich, N.C., Improta, T., Baxter, G., Daniel-Issakani, S., Strulovici, B., 1991. Transmembrane signaling by interferon alpha involves diacylglycerol production and activation of the epsilon isoform of protein kinase C in Daudi cells. Proc. Nat. Acad. Sci. U.S.A. 88, 7988–7992.
Pfeffer, L.M., Strulovici, B., Saltiel, A.R., 1990. Interferon-alpha selectively activates the beta isoform of protein kinase C through phosphatidylcholine hydrolysis. Proc. Nat. Acad. Sci. U.S.A. 87, 6537–6541.
Rafty, L.A., Khachigian, L.M., 2001. Sp1 phosphorylation regulates inducible expression of platelet-derived growth factor B-chain gene via atypical protein kinase C-zeta. Nucleic Acids Res. 29, 1027–1033.
Raney, A.K., Johnson, J.L., Palmer, C.N., McLachlan, A., 1997. Members of the nuclear receptor superfamily regulate transcription from the hepatitis B virus nucleocapsid promoter. J. Virol. 71, 1058–1071.
Rang, A., Heise, T., Will, H., 2001. Lack of a role of the interferon-stimulated response element-like region in interferon alpha -induced suppression of Hepatitis B virus in vitro. J. Biol. Chem. 276, 3531–3535.
Romero, R., Lavine, J.E., 1996. Cytokine inhibition of the hepatitis B virus core promoter. Hepatology 23, 17–23.
Schulte-Frohlinde, E., Seidler, B., Burkard, I., Freilinger, T., Lersch, C., Erfle, V., Foster, G.R., Classen, M., 2002. Different activities of type I interferons on hepatitis B virus core promoter regulated transcription. Cytokine 17, 214–220.
Srivastava, K.K., Batra, S., Sassano, A., Li, Y., Majchrzak, B., Kiyokawa, H., Altman, A., Fish, E.N., Platanias, L.C., 2004. Engagement of protein kinase C-theta in interferon signaling in T-cells. J. Biol. Chem. 279, 29911–29920.
Su, H., Yee, J.K., 1992. Regulation of hepatitis B virus gene expression by its two enhancers. Proc. Nat. Acad. Sci. U.S.A. 89, 2708–2712.
Sureau, C., Romet-Lemonne, J.L., Mullins, J.I., Essex, M., 1986. Production of hepatitis B virus by a differentiated human hepatoma cell line after transfection with cloned circular HBV DNA. Cell 47, 37–47.
Tur-Kaspa, R., Teicher, L., Laub, O., Itin, A., Dagan, D., Bloom, B.R., Shafritz, D.A., 1990. Alpha interferon suppresses hepatitis B virus enhancer activity and reduces viral gene transcription. J. Virol. 64, 1821–1824.
Uddin, S., Sassano, A., Deb, D.K., Verma, A., Majchrzak, B., Rahman, A., Malik, A.B., Fish, E.N., Platanias, L.C., 2002. Protein kinase C-delta (PKC-delta) is activated by type I interferons and mediates phosphorylation of Stat1 on serine 727. J. Biol. Chem. 277, 14408–14416.
Uddin, S., Yenush, L., Sun, X.J., Sweet, M.E., White, M.F., Platanias, L.C., 1995. Interferon-alpha engages the insulin receptor substrate-1 to associate with the phosphatidylinositol 3′-kinase. J. Biol. Chem. 270, 15938–15941.
Vannice, J.L., Levinson, A.D., 1988. Properties of the human hepatitis B virus enhancer: position effects and cell-type nonspecificity. J. Virol. 62, 1305–1313.
von Hahn, T., Schulze, A., Chicano Wust, I., Heidrich, B., Becker, T., Steinmann, E., Helfritz, F.A., Rohrmann, K., Urban, S., Manns, M.P., Pietschmann, T., Ciesek, S., 2011. The novel immunosuppressive protein kinase C inhibitor sotrastaurin has no pro-viral effects on the replication cycle of hepatitis B or C virus. PLoS One 6, e24142.
Wang, W.X., Li, M., Wu, X., Wang, Y., Li, Z.P., 1998. HNF1 is critical for the liver-specific function of HBV enhancer II. Res. Virol. 149, 99–108.
Wang, Y., Chen, P., Wu, X., Sun, A.L., Wang, H., Zhu, Y.A., Li, Z.P., 1990. A new enhancer element, ENII, identified in the X gene of hepatitis B virus. J. Virol. 64, 3977–3981.
Yee, J.K., 1989. A liver-specific enhancer in the core promoter region of human hepatitis B virus. Science 246, 658–661.
Yuh, C.H., Ting, L.P., 1990. The genome of hepatitis B virus contains a second enhancer: cooperation of two elements within this enhancer is required for its function. J. Virol. 64, 4281–4287.
Yuh, C.H., Ting, L.P., 1991. C/EBP-like proteins binding to the functional box-alpha and box-beta of the second enhancer of hepatitis B virus. Mol. Cell. Biol. 11, 5044–5052.

Dynamics of Hepatitis B Virus Quasispecies in Association with Nucleos(t)ide Analogue Treatment Determined by Ultra-Deep Sequencing

Norihiro Nishijima[1], Hiroyuki Marusawa[1]*, Yoshihide Ueda[1], Ken Takahashi[1], Akihiro Nasu[1], Yukio Osaki[2], Tadayuki Kou[3], Shujiro Yazumi[3], Takeshi Fujiwara[4], Soken Tsuchiya[4], Kazuharu Shimizu[4], Shinji Uemoto[5], Tsutomu Chiba[1]

1 Department of Gastroenterology and Hepatology, Graduate School of Medicine, Kyoto University, Kyoto, Japan, **2** Department of Gastroenterology and Hepatology, Osaka Red Cross Hospital, Osaka, Japan, **3** Department of Gastroenterology and Hepatology, Tazuke Kofukai Medical Research Institute, Kitano Hospital, Osaka, Japan, **4** Department of Nanobio Drug Discovery, Graduate School of Pharmaceutical Sciences, Kyoto University, Kyoto, Japan, **5** Department of Surgery, Graduate School of Medicine, Kyoto University, Kyoto, Japan

Abstract

Background and Aims: Although the advent of ultra-deep sequencing technology allows for the analysis of heretofore-undetectable minor viral mutants, a limited amount of information is currently available regarding the clinical implications of hepatitis B virus (HBV) genomic heterogeneity.

Methods: To characterize the HBV genetic heterogeneity in association with anti-viral therapy, we performed ultra-deep sequencing of full-genome HBV in the liver and serum of 19 patients with chronic viral infection, including 14 therapy-naïve and 5 nucleos(t)ide analogue(NA)-treated cases.

Results: Most genomic changes observed in viral variants were single base substitutions and were widely distributed throughout the HBV genome. Four of eight (50%) chronic therapy-naïve HBeAg-negative patients showed a relatively low prevalence of the G1896A pre-core (pre-C) mutant in the liver tissues, suggesting that other mutations were involved in their HBeAg seroconversion. Interestingly, liver tissues in 4 of 5 (80%) of the chronic NA-treated anti-HBe-positive cases had extremely low levels of the G1896A pre-C mutant (0.0%, 0.0%, 0.1%, and 1.1%), suggesting the high sensitivity of the G1896A pre-C mutant to NA. Moreover, various abundances of clones resistant to NA were common in both the liver and serum of treatment-naïve patients, and the proportion of M204VI mutants resistant to lamivudine and entecavir expanded in response to entecavir treatment in the serum of 35.7% (5/14) of patients, suggesting the putative risk of developing drug resistance to NA.

Conclusion: Our findings illustrate the strong advantage of deep sequencing on viral genome as a tool for dissecting the pathophysiology of HBV infection.

Citation: Nishijima N, Marusawa H, Ueda Y, Takahashi K, Nasu A, et al. (2012) Dynamics of Hepatitis B Virus Quasispecies in Association with Nucleos(t)ide Analogue Treatment Determined by Ultra-Deep Sequencing. PLoS ONE 7(4): e35052. doi:10.1371/journal.pone.0035052

Editor: Antonio Bertoletti, Singapore Institute for Clinical Sciences, Singapore

Received November 17, 2011; **Accepted** March 8, 2012; **Published** April 16, 2012

Funding: This work was supported by JSPS Grant-in-aid for Scientific Research 21229009, 23390196, and Health and Labor Science Research Grants (H22-08) and Research on Hepatitis from the Ministry of Health, Labor and Welfare, Japan. (http://mhlw-grants.niph.go.jp/). The funders had no role in study design, data collection and analysis, decision to publish, or preparation of the manuscript.

Competing Interests: The authors have declared that no competing interests exist.

* E-mail: maru@kuhp.kyoto-u.ac.jp

Introduction

Hepatitis B virus (HBV) is a non-cytopathic DNA virus that infects approximately 350 million people worldwide and is a main cause of liver-related morbidity and mortality [1–3]. The absence of viral-encoded RNA-dependent DNA polymerase proofreading capacity coupled with the extremely high rate of HBV replication yields the potential to rapidly generate mutations at each nucleotide position within the entire genome [4]. Accordingly, a highly characteristic nature of HBV infection is the remarkable genetic heterogeneity at the inter- and intra- patient level. The latter case of variability as a population of closely-related but nonidentical genomes is referred to as viral quasispecies [5,6]. It is well recognized that such mutations may have important implications regarding the pathogenesis of viral disease. For example, in chronic infection, G to A point mutation at nucleotide (nt) 1896 in the pre-core (pre-C) region as well as A1762T and G1764A mutations in the core-promoter region are highly associated with HBeAg seroconversion that in general results in the low levels of viremia and consequent clinical cure [7–9]. In contrast, acute infection with the G1896A pre-C mutant represents a high risk for fulminant hepatic failure [10,11]. Although these facts clearly illustrate the clinical implications of certain viral mutation, increasing evidence strongly suggests that

the viral genetic heterogeneity is more complicated than previously thought [12,13].

The major goals of antiviral therapy in patients with HBV infection are to prevent the progression of liver disease and inhibit the development of hepatocellular carcinoma [14]. Oral nucleos(t)ide analogue (NA) have revolutionized the management of HBV infection, and five such antiviral drugs, including lamivudine, adefovir, entecavir, tenofovir, and telbivudine, are currently approved medications [15,16]. These agents are well-tolerated, very effective at suppressing viral replication, and safe, but one of the major problems of NA therapy is that long-term use of these drugs frequently causes the emergence of antiviral drug-resistant HBV due to substitutions at specific sites in the viral genome sequences, which often negates the benefits of therapy and is associated with hepatitis flares and death [16,17]. It is unclear whether viral clones with antiviral resistance emerge after the administration of antiviral therapy or widely preexist among treatment-naïve patients.

There has been a recent advance in DNA sequencing technology [18]. The ultra-deep sequencers allow for massively parallel amplification and detection of sequences of hundreds of thousands of individual molecules. We recently demonstrated the usefulness of ultra-deep sequencing technology to unveil the massive genetic heterogeneity of hepatitis C virus (HCV) in association with treatment response to antiviral therapy [19]. On the other hand, there are a few published studies in which this technology was used to characterize genetic HBV sequence variations [20–22]. Margeridon-Thermet et al reported that the 454 Life Science GS20 sequencing platform provided higher sensitivity for detecting drug-resistant HBV mutations in the serum of patients treated with nucleoside and nucleotide reverse-transcriptase inhibitors [20]. Solmone et al also reported the strong advantage conferred by the same platform to detect minor variants in the serum of patients with chronic HBV infection [21]. Although in these previous studies low-abundant drug-resistant variants were successfully detected, the analyses were focused on the reverse-transcriptase region of circulating HBV in the serum and thus the whole picture of HBV genetic heterogeneity as well as the *in vivo* dynamics of HBV drug resistant variants in response to anti-viral treatment remains to be clarified. Moreover, intrahepatic viral heterogeneity in patients that achieved the clearance of circulating HBV is largely unknown.

By taking the advantage of an abundance of genetic information obtained by utilizing the Illumina Genome Analyzer II (Illumina, San Diego, CA) as a platform of ultra-deep sequencing, we determined the whole HBV sequence in the liver and serum of patients with chronic HBV infection to evaluate viral quasispecies characteristics. Moreover, we investigated the prevalence of rare drug-resistant HBV variants as well as detailed dynamic changes in the viral genetic heterogeneity in association with NA administration. Based on the abundant genetic information obtained by ultra-deep sequencing, we clarified the precise prevalence of HBV clones with G1896A pre-C mutations in association with HBe serostatus in chronically infected patients with or without NA treatment. We also detected a variety of minor drug-resistant clones in treatment-naïve patients and their dynamic changes in response to entecavir administration, demonstrating the potential clinical significance of naturally-occurring drug-resistant mutations.

Materials and Methods

Ethics Statement

The Kyoto University ethics committee approved the study, and written informed consent for participation in this study was obtained from all patients. The study was conducted in accordance with the principles of the Declaration of Helsinki.

Patients

The liver tissues of 19 Japanese patients that underwent living-donor liver transplantation at Kyoto University due to HBV-related liver disease were available for viral genome analyses. These individuals included 13 men and 6 women, aged 41 to 69 years (median, 55.2 years) and all but one were infected with genotype C viruses. Participants comprised 19 patients with liver cirrhosis caused by chronic HBV infection, including 14 antiviral therapy-naïve cases (chronic-naïve cases) and 5 cases receiving NA treatment, with either lamivudine or entecavir (chronic-NA cases) (Table 1). Serum HBV DNA levels were significantly higher in chronic-naïve cases than in chronic NA cases (median serum HBV DNA levels were 5.6, and <2.6 log copies/ml, respectively, Table 1). Liver tissue samples were obtained at the time of transplantation, frozen immediately, and stored at −80°C until use. Serologic analyses of HBV markers, including hepatitis B surface antigen (HBsAg), antibodies to HBsAg, anti-HBc, HBeAg, and antibodies to HBeAg, were determined by enzyme immunoassay kits as described previously [23]. HBV DNA in the serum before transplantation was examined using a polymerase chain reaction (PCR) assay (Amplicor HBV Monitor, Roche, Branchburg, NJ). To examine the dynamics of viral quasispecies in response to anti-HBV therapy, paired serum samples of 14 treatment-naïve patients before and after administration of daily entecavir (0.5 mg/day) were subjected to further analyses on viral genome.

Direct population Sanger sequencing

DNA was extracted from the liver tissue and serum using a DNeasy Blood & Tissue Kit (Qiagen, Tokyo, Japan). To define the consensus reference sequences of HBV in each clinical specimen, all samples were first subjected to direct population Sanger sequencing using the Applied Biosystems 3500 Genetic Analyzer (Applied Biosystems, Foster City, CA). Oligonucleotide primers for the HBV genome were designed to specifically amplify whole viral sequences as two overlapping fragments using the sense primer 169_F and antisense primer 2847_R to yield a 2679-bp amplicon (amplicon 1), and the sense primer 685_F and antisense primer 443_R to yield a 2974-bp amplicon (amplicon 2; Table S1). HBV sequences were amplified using Phusion High-Fidelity DNA polymerase (FINZYMES, Espoo, Finland). All amplified PCR products were purified using the QIAquick Gel Extraction kit (Qiagen) after agarose gel electrophoresis and used for direct sequencing. The serum of a healthy HBV DNA-negative volunteer was used as a negative control.

Viral genome sequencing by massively-parallel sequencing

Massively-parallel sequencing with multiplexed tags was performed using the Illumina Genome Analyzer II as described [19]. The end-repair of DNA fragments, addition of adenine to the 3′ ends of DNA fragments, adaptor ligation, and PCR amplification by Illumina PCR primers were performed as described previously [24]. Briefly, the viral genome sequences were amplified by high-fidelity PCR using oligonucleotide primers as described above, sheared by nebulization using 32 psi N2 for 8 min, and then the sheared fragments were purified and concentrated using a QIAquick PCR purification Kit (Qiagen). Nucleotide overhangs resulting from fragmentation were then converted into blunt ends using T4 DNA polymerase and Klenow

Table 1. Characteristics of patients with chronic HBV infection analyzed in this study.

	Chronic-naïve (N = 14)	Chronic-NA (N = 5)
Age†	55.5 (41–69)	55.0 (49–68)
Sex (male/female)	9/5	4/1
Alanine aminotransaminase (IU/l)†	41 (10–74)	30 (15–65)
Total bilirubin (mg/dl)†	0.9 (0.5–31.1)	1.7 (0.6–4.5)
Platelet count ($\times 10^4/mm^3$)†	12.7 (3.3–27.6)	5.1 (3.6–11.3)
HBV genotype		
B	1	0
C	13	5
Viral load (log copies /ml)†	5.6 (<2.6–8.8)*	<2.6 (<2.6–5.3)*
HBe-serostatus (HBeAg+/HBeAb+)	8/6	0/5
Fibrosis		
F0–F2	6	0
F3–F4	8	5
Activity		
A0–A1	7	3
A2–A3	7	2

†Values are median (range).
*P = 0.042.
doi:10.1371/journal.pone.0035052.t001

enzymes, followed by the addition of terminal 3′ A-residues. An adaptor containing unique 6-bp tags, such as "ATCACG" and "CGATGT" (Multiplexing Sample Preparation Oligonucleotide Kit, Illumina), was then ligated to each fragment using DNA ligase. We then performed agarose gel electrophoresis of adaptor-ligated DNAs and excised bands from the gel to produce libraries with insert sizes ranging from 200 to 350 bp. These libraries were amplified independently using a minimal PCR amplification step of 18 cycles by Illumina PCR primers with Phusion High-Fidelity DNA polymerase. The DNA fragments were then purified with a MinElute PCR Purification Kit (Qiagen), followed by quantification using the NanoDrop 2000C (Thermo Fisher Scientific, Waltham, MA) to make a working concentration of 10 nM. Cluster generation and sequencing was performed for 64 cycles on the Illumina Genome Analyzer II according to the manufacturer's instructions. The obtained images were analyzed and base-called using GA pipeline software version 1.4 with the default settings provided by Illumina.

Genome Analyzer sequence data analysis

Using the high performance alignment software "NextGene" (SoftGenetics, State College, PA), the 64 base-pair reads obtained from the Genome Analyzer II were aligned with the reference sequences of 3215 bp that were determined by direct population Sanger sequencing of each clinical specimen. Reads with 90% or more bases matching a particular position of the reference sequences were aligned. Furthermore, two quality filters were used for sequencing reads: the reads with a median quality score of more than 30 and no more than 3 uncalled nucleotides were allowed anywhere in the 64 bases. Only sequences that passed the quality filters, rather than raw sequences, were analyzed and each position of the viral genome was assigned a coverage depth, representing the number of times the nucleotide position was sequenced.

Allele-specific quantitative real-time PCR and semiquantitative PCR to determine the relative proportion of G1896A pre-C mutant

To determine the relative proportion of the G1896A pre-C mutant, allele-specific quantitative real-time PCR was performed based on the previously described method [25,26]. Oligonucleotide primers were designed individually to amplify the pre-C region of wild-type and the G1896A pre-C mutant HBV. Three primers were used for this protocol, two allele-specific sense primers, 1896WT_F (for wild-type) and 1896MT_F (for the G1896A pre-C mutant), and one common antisense primer, 2037_R (Table S1). Quantification of wild-type and the G1896A pre-C mutant was individually performed by real-time PCR using a Light Cycler 480 and Fast Start Universal SYBR Master (Roche, Mannheim, Germany) [27]. The relative proportion of the G1896A pre-C mutant was determined to calculate the G1896A pre-C mutant/total HBV ratios. Performance of this assay was tested using mixtures of two previously described plasmids, pcDNA3-HBV-wt#1 and pcDNA3-HBV-G1896A pre-C mutant [28]. Semiquantitative PCR was performed using primers described above, then agarose gel electrophoresis was performed.

Statistical analysis

Results are expressed as mean or median, and range. Pretreatment values were compared using the Mann-Whitney U-test or the Kruskal Wallis H-test. *P* values less than 0.05 were considered statistically significant.

The viral quasispecies characteristics were evaluated by analyzing the genetic complexity based on the number of different sequences present in the population. Genetic complexity for each site was determined by calculating the Shannon entropy using the following formula:

$$Sn = -\frac{\sum_{i=1}^{n} fi(lnfi)}{N}$$

where n is the number of different species identified, f_i is the observed frequency of a particular variant in the quasispecies, and N is the total number of clones analyzed [12,13]. The mean viral complexity in each sample was determined by calculating the total amounts of the Shannon entropy at each nucleotide position divided by the total nucleotide number (e.g., 3215 bases) of each HBV genome sequence.

Nucleotide sequence accession number

All sequence reads have been deposit in DNA Data Bank of Japan Sequence Read Archive (http://www.ddbj.nig.ac.jp/index-e.html) under accession number DRA000435.

Results

Validation of multiplex ultra-deep sequencing of the HBV genome

To differentiate true mutations from sequencing errors in the determined sequences, we first generated viral sequence data from the expression plasmid, pcDNA3-HBV-wt#1, encoding wild-type genotype C HBV genome sequences [28]. For this purpose, we determined the PCR-amplified HBV sequences derived from the expression plasmid using high-fidelity Taq polymerase to take the PCR-induced errors as well as sequencing errors into consideration. Viral sequences determined by the conventional Sanger method were used as reference sequences for aligning the amplicons obtained by ultra-deep sequencing. Three repeated ultra-deep sequencing generated a mean of 77,663 filtered reads, corresponding to a mean coverage of 38,234 fold at each nucleotide site (Table S2). Errors comprised insertions (0.00003%), deletions (0.00135%), and nucleotide mismatches (0.037%). The mean overall error rate was 0.034% (distribution of per-nucleotide error rate ranged from 0 to 0.13%) for the three control experiments, reflecting the error introduced by high-fidelity PCR amplification and by multiplex ultra-deep sequencing that remained after filtering out problematic sequences. We also confirmed that multiplex ultra-deep sequencing with and without the high-fidelity PCR amplification with HBV-specific primer sets showed no significant differences in the error rates on the viral sequence data (mean error rate 0.034% vs 0.043%). Accordingly, we defined the cut-off value in its current platform as 0.3%, a value nearly 1 log above the mean overall error rate.

Next, we performed additional control experiments to verify the detectability of the low abundant mutations that presented at a frequency of less than 0.3%. For this purpose, we introduced expression plasmids with a single-point mutation within that encoding a wild-type viral sequence with a ratio of 1:1000 and assessed the sensitivity and accuracy of quantification using high-fidelity PCR amplification followed by multiplex ultra-deep sequencing in association with the different coverage numbers (Table S3). Repeated control experiments revealed that the threshold for detecting low-abundant mutations at an input ratio of 0.10% among the wild-type sequences ranged between 0.11% and 0.24%, indicating that there was no significant difference in the detection rate or error rates under the different coverage conditions. Based on these results, the accuracy of ultra-deep sequencing in its current platform for detecting low-level viral mutations was considered to be greater than 0.30%.

Viral complexity of the HBV quasispecies in association with clinical status

To clarify HBV quasispecies in association with clinical status, we performed multiplex ultra-deep sequencing and determined the HBV full-genome sequences in the liver and serum with chronic HBV infection. First, we compared the sequences of the viral genome determined in the liver tissue with those in the serum and found no significant differences in the viral population between the liver and serum of the same individual. Indeed, the pattern and distribution of genetic heterogeneity of the viral nucleotide sequences in the liver tissue were similar to those observed in the serum of the same patient (Figure S1), suggesting that a similar pattern of viral heterogeneity was maintained in the liver and serum of patients with chronic HBV infection.

Next, we compared the viral heterogeneity in the liver of chronic-naïve and chronic-NA cases. A mean of 5,962,996 bp nucleotides in chronic-naïve cases and 4,866,783 bp nucleotides in chronic-NA cases were mapped onto the reference sequences, and an overall average coverage depth of 1,855 and 1.514 was achieved for each nucleotide site of the HBV sequences, respectively (Table 2). The frequencies of mutated positions and altered sequence variations detected in each viral genomic region are summarized in Table 2. The overall mutation frequency of the total viral genomic sequences was determined to be 0.87% in chronic-naïve cases and 0.69% in chronic-NA cases. Most genomic changes observed in viral variants were single base substitutions, and the genetic heterogeneity of the viral nucleotide sequences was equally observed throughout the individual viral genetic regions, including the pre-surface (preS), S, pre-core~core (preC-C), and X (Table 2). Consistent with the findings obtained from the viral mutation analyses, the overall viral complexity determined by the Shannon entropy value was 0.047 in chronic-naïve and 0.036 in chronic-NA cases, and the viral complexity was equally observed throughout the individual viral genetic region (Figure 1A). Among chronic-naïve cases, we observed no significant differences in the viral complexity in HBV DNA level, age, or degree of fibrosis (Figure 1B).

High sensitivity of the G1896A pre-C mutant to nucleos(t)ide analogues

Emergence of G1896A mutation in the pre-C region, and A1762T and G1764A mutations in the core-promoter region is well known to be associated with HBe-seroconversion [7–9]. We then evaluated the prevalence of these three mutations in the chronically HBV-infected liver, in association with HBe serologic status and the NA treatment history. In chronic-naive cases, 6 and 8 patients showed the pre- and post- HBeAg seroconversion status, respectively (Table 3). The mean prevalence of the G1896A pre-C mutant in HBeAg-positive cases was lower than that in the HBeAg-negative cases (27.4% and 46.5%, respectively). Importantly, however, 4 of 8 HBeAg-negative cases showed a relatively low prevalence of the G1896A pre-C mutant (Liver #8, #12, #13, #14), and all but one case (Liver #10) showed a high prevalence of the A1762T and G1764A mutations, irrespective of HBe serologic status and NA treatment history (Table 3). These findings suggested that other mutations except G1896A, A1762T and G1764A were also involved in the HBeAg seroconversion status. Notably, liver tissues of all but one (Liver #17) chronic-NA cases showed extremely low levels of the G1896A pre-C mutant (0.0, 0.0, 0.1, and 1.1%), suggesting the high sensitivity of the G1896A pre-C mutant to NA (Table 3).

To confirm the difference of the sensitivity to NA between the wild-type and the G1896A pre-C mutant, we examined the dynamic changes of the relative proportion of the G1896A pre-C mutant in the serum of 14 treatment-naïve patients before and after entecavir administration. Consistent with the findings obtained by ultra-deep sequencing, quantitative real-time PCR revealed that entecavir administration significantly reduced the proportion of the G1896A pre-C mutant in 13 of 14 cases (92.9%)

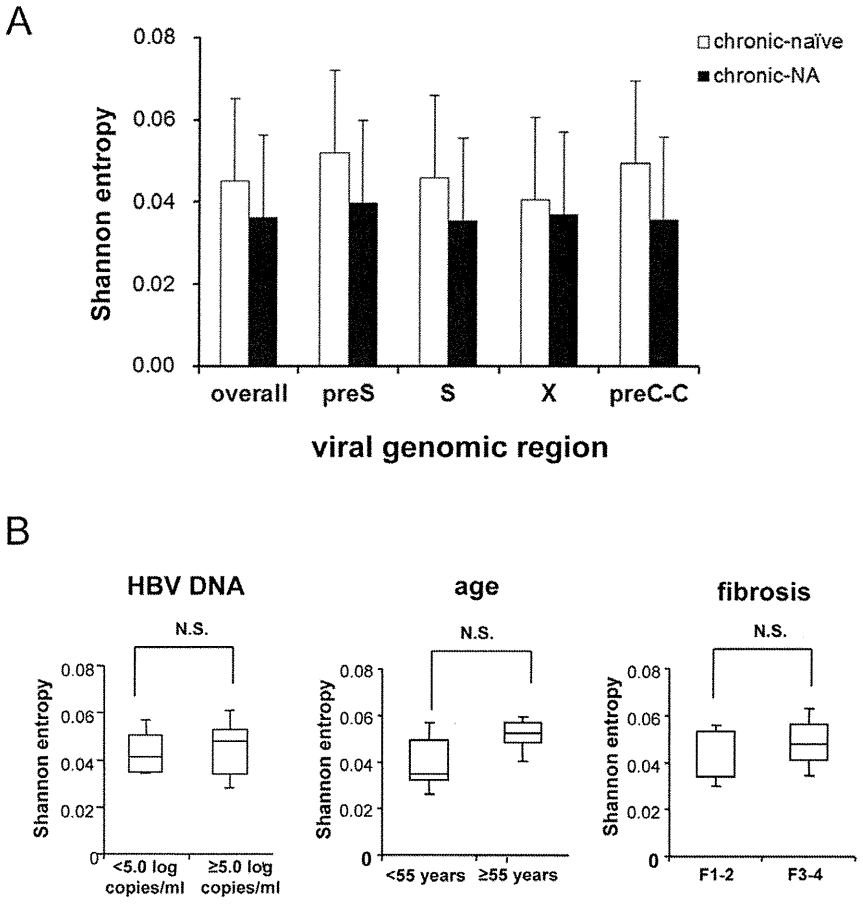

Figure 1. Viral complexity of the HBV quasispecies in association with clinical status. (A) The Shannon entropy values for each viral genomic region were determined in the liver of chronic-naïve and chronic-NA cases. (B) Among the chronic-naïve cases, the Shannon entropy values are shown for patients with serum HBV DNA levels less than 5.0 log copies/ml (<5.0) and greater than 5.0 log copies/ml (≥5.0) (left panel), patients under the age of 55 years (<55) and over the age of 55 (≥55) (middle panel), and patients with low (F1–2) and high (F3–4) liver fibrosis levels (right panel). preS: pre-surface, preC-C: precore~core N.S.: not significant.
doi:10.1371/journal.pone.0035052.g001

Table 2. The frequency of mutation rate and the Shannon entropy in each viral genome region.

	Liver	
	Chronic-naïve (N = 14)	**Chronic-NA (N = 5)**
Average aligned reads	93,172	76,043
Average aligned nucleotides	5,962,996	4,866,783
Average coverage	1,855	1,514
Mutation rate (%)		
Overall	0.87	0.69
preS	0.92	0.81
S	0.96	0.71
preC-C	1.05	0.72
X	0.63	0.61
Shannon entropy	0.047	0.036

Mutation rate (%): the ratio of total different nucleotides from the reference sequence to total aligned nucleotides.
preS: pre-surface, preC-C: pre-core~core.
doi:10.1371/journal.pone.0035052.t002

irrespective of their HBeAg serostatus, while the G1896A pre-C mutant were detectable in substantial proportion before treatment in all cases (Figure 2A, 2B and 2C; $p = 0.001$). These results further support the findings that HBV clones comprising the G1896A mutation were more sensitive to NA than those with wild-type sequences.

Prevalence of drug-resistant HBV clones in the liver of treatment-naïve patients

Increasing evidence suggests that drug-resistant viral mutants can be detected in the serum of treatment-naïve patients with chronic HBV infection [20,21]. Thus, we next determined the actual prevalence of spontaneously-developed drug-resistant mutants in chronically-infected liver of treatment-naïve patients to evaluate whether NA treatment potentiates the expansion of drug-resistant clones. The drug-resistant mutations examined included two mutations resistant to lamivudine and entecavir, four mutations resistant to entecavir, and three mutations resistant to adefovir [16,17]. Based on the detection rate of the low-level viral clones determined by the control experiments, we identified the drug-resistant mutants present in each specimen at a frequency of more than 0.3% among the total viral clones. Based on these criteria, at least one resistant mutation was detected in the liver of all of the chronic-naïve cases with chronic HBV infection (Table 4).

Table 3. The prevalence of G1896A mutation in the pre-C region, and A1762T and G1764A mutations in the core-promoter region in the liver of patients chronically infected with HBV.

			Mutation Frequency					
	HBeAg/HBeAb	NA (duration of treatment)	G1896A (Pre C)		A1762T (CP)		G1764A (CP)	
Chronic-naive								
Liver #1	+/−	-	640/1652	(38.7)	1647/1941	(84.9)	1683/1979	(85.0)
Liver #2	+/−	-	9/596	(1.5)	682/687	(99.3)	683/689	(99.1)
Liver #3	+/−	-	273/672	(40.6)	767/769	(99.7)	757/760	(99.6)
Liver #4	+/−	-	204/701	(29.1)	610/625	(97.6)	602/621	(96.9)
Liver #5	+/−	-	27/152	(17.8)	249/250	(99.6)	245/248	(98.8)
Liver #6	+/−	-	228/621	(36.7)	727/729	(99.7)	743/744	(99.9)
Liver #7	−/+	-	740/1193	(62.0)	1908/1913	(99.7)	1888/1913	(98.7)
Liver #8	−/+	-	111/1892	(5.9)	2321/2325	(99.8)	2335/2339	(99.8)
Liver #9	−/+	-	10935/10944	(99.9)	12019/12032	(99.9)	12163/12170	(99.9)
Liver #10	−/+	-	4554/4593	(99.2)	1/5191	(0)	4/5188	(0.1)
Liver #11	−/+	-	811/921	(88.1)	1234/1236	(99.8)	1226/1228	(99.8)
Liver #12	−/+	-	93/1265	(7.4)	1234/1234	(100)	1228/1229	(99.9)
Liver #13	−/+	-	83/877	(9.5)	1465/1529	(95.8)	1485/1549	(95.9)
Liver #14	−/+	-	0/717	(0)	1078/1410	(76.5)	1089/1414	(77.0)
Chronic-NA								
Liver #15	−/+	LAM (156w)	0/390	(0)	441/453	(97.4)	435/448	(97.1)
Liver #16	−/+	ETV (1w)	0/1399	(0)	1624/1632	(99.5)	1625/1630	(99.7)
Liver #17	−/+	LAM (144w)	345/816	(42.3)	988/991	(99.7)	994/994	(100)
Liver #18	−/+	LAM (98w)	2/3963	(0.1)	1015/1188	(85.4)	1190/1194	(99.7)
Liver #19	−/+	LAM (11w)	48/4214	(1.1)	3438/3456	(99.5)	3446/3462	(99.5)

Values in parenthesis show mutation frequency (%): the ratio of total mutant clones to total aligned coverage at each nucleotide sites.
NA: nucleotide analogue, pre C: precore, CP: core promoter, LAM: lamivudine, ETV: entecavir.
doi:10.1371/journal.pone.0035052.t003

The prevalence of the 9 drug-resistant mutations detected by ultra-deep sequencing in 14 chronic-naïve cases ranged from 0.3% to 30.0%, indicating that the proportion of resistant mutations substantially differed in each case. The most commonly detected mutation was M204VI (9 cases) and M250VI (11 cases), which were resistant to lamivudine and entecavir, and entecavir, respectively. Other mutations resistant to adefovir were detected in 7 (50.0%) and 3 (21.4%) cases at A181TV and N236T, respectively (Table 4).

Nine (64.2%) chronic-naïve cases possessed the M204VI mutants in their liver tissues and the proportion of mutant clones among the totally infected viruses ranged from 0.3% to 1.1% among the M204VI mutant-positive patients. In chronic-NA cases, 4 of 5 (80.0%) liver tissues harbored the M204VI mutants with the proportion among the totally infected viruses ranging from 0.4% to 18.7% (Table 4), while the mean serum HBV DNA was suppressed below 2.6 log copies/ml (Table 1). These results suggest that the mutant HBV clones comprising various drug-resistant mutations could latently exist even in the liver of NA treatment-naïve cases.

Expansion of drug-resistant HBV clones harboring M240VI mutations in response to NA administration

To clarify the risk of latent expansion of drug-resistant mutations due to NA treatment, we next examined the early dynamic changes of the prevalence of M204VI mutants in the serum of treatment-naïve patients in response to entecavir treatment. Ultra-deep sequencing provided a mean 40,791- and 38,823-fold coverage of readings, which were mapped to the M204VI nucleotide position at the YMDD sites of each reference sequence in patients before and after entecavir treatment.

Five of 14 (35.7%) patients harbored the M204VI mutations prior to entecavir treatment. Although the serum HBV DNA levels were significantly reduced in response to entecavir in all cases, the M204VI mutant clones were detected in 9 cases (64.3%) after entecavir administration (Table 5). Notably, one patient (Serum #3) who harbored the M240VI mutant clones at baseline had a relatively large expansion of drug-resistant clones among the total viral population in a time-dependent manner in response to entecavir treatment (Table 5). Similarly, M240VI mutant clones became detectable after entecavir administration in four patients (Serum #1, #7, #12, #13) that harbored no resistant mutants at baseline (Table 5). We found no correlation between the degree of the increase in the relative prevalence of M204VI mutant clones and that of the reduction in serum HBV DNA levels. Although only a limited number of patients exhibited a substantial increase in M204VI mutant clones after administration of anti-viral therapy, our findings might suggest that entecavir treatment latently causes selective survival of drug-resistant mutants in treatment naïve patients with chronic HBV infection.

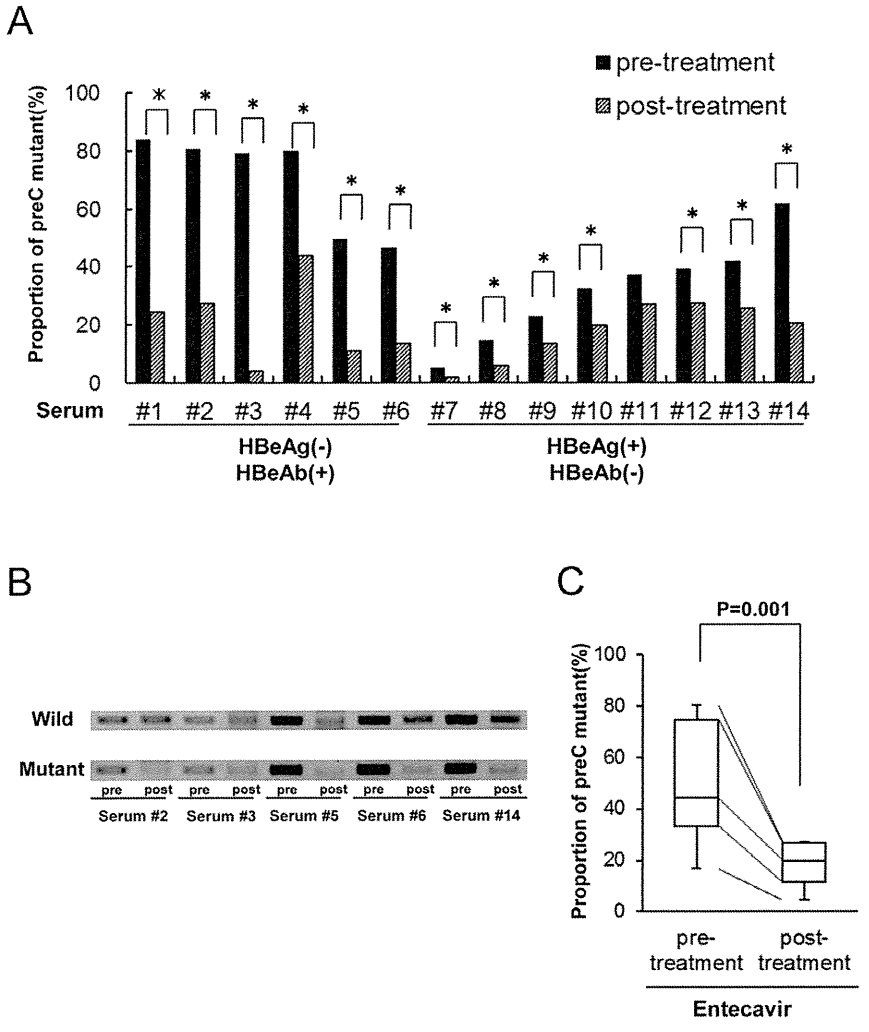

Figure 2. The reduction in the relative proportion of the G1896A pre-C mutant clones after entecavir administration. (A) The relative proportion of the G1896A pre-C mutant was determined in the serum of treatment-naïve patients pre- and post-entecavir administration using quantitative real-time PCR. Serum #1~6 were HBeAg-negative and HBeAb-positive, and Serum #7~14 were HBeAg-positive and HBeAb-negative before treatment. *: $p<0.05$ (B) Semiquantitative PCR analysis was performed using primers specific to the wild-type (upper panel) or G1896A pre-C mutant (lower panel) pre- and post-entecavir administration. A representative result from 5 cases is shown. (C) The relative proportion of the G1896A pre-C mutant was compared in 14 treatment-naïve patients between pre- and post-entecavir administration.
doi:10.1371/journal.pone.0035052.g002

Discussion

Direct population sequencing is the most common method for detecting viral mutations [29]. Conventional sequencing techniques, however, are not efficient for evaluating large amounts of genetic information of the viruses. Newly developed ultra-deep sequencing technology have revolutionized genomic analyses, allowing for studies of the dynamics of viral quasispecies as well as rare genetic variants of the viruses that cannot be detected using standard direct population sequencing techniques [30,31]. The sensitivity of ultra-deep sequencing analysis is primarily limited by errors introduced during PCR amplification and the sequencing reaction, thus it is a challenge to distinguish rare variants from sequencing artifacts. In the present study, we optimized the ultra-deep sequencing with a multiplex-tagging method and reproducibly detected variants within HBV quasispecies that were as rare as 0.3%. Based on this ultra-deep sequencing platform, we determined the abundant genetic heterogeneity of HBV at the intra- and inter-individual levels.

Because of its ability to handle abundant viral genome information, ultra-deep sequencing allowed us to evaluate low-abundant virus variants of patients with chronic HBV infection in detail. It is widely accepted that HBe seroconversion is highly associated with the emergence of G1896A pre-C and/or A1762T and G1764A core promoter mutant clones [7–9]. Unexpectedly, however, our results showed a diverse range of G1896A frequency (0–99.9%) in HBeAg-negative subjects and a high prevalence of core promoter mutations, irrespective of HBe serostatus. Consistent with our observation, previous studies utilizing conventional sequencing methods reported that the frequency of the G1896A pre-C mutant ranged from 12% to 85% [32]. All but one patient (Liver #10) showing a predominance of A1762T and G1764A were infected with genotype C, while patient#10 was infected with genotype B. Because A1762T and G1764A are reported to be significantly more frequent in genotype C [33], the difference in the prevalence of A1762T and G1764A in our study might be a reflection of the viral HBV genotype rather than HBe serostatus. Further investigation of the actual prevalence of these mutations

Table 4. The prevalence of the 9 drug-resistant mutations detected by ultra-deep sequencing derived from liver tissue.

	M204V/I		L180M		T184S/A/I/ L/G/C/M		S202C/G/I		I169T	
Drugs	**LAM/ETV**		**LAM/ETV**		**ETV**		**ETV**		**ETV**	
Chronic-naive										
Liver #1	**27/5421**	**(0.5%)**	2/3694	(-)	9/3886	(-)	5/5613	(-)	5/3784	(-)
Liver #2	**35/5344**	**(0.7%)**	0/538	(-)	1/563	(-)	17/6340	(-)	0/512	(-)
Liver #3	**13/1363**	**(1.0%)**	0/304	(-)	1/358	(-)	1/1379	(-)	0/264	(-)
Liver #4	11/5113	(-)	0/556	(-)	**2/547**	**(0.4%)**	11/5133	(-)	0/639	(-)
Liver #5	**2/117**	**(1.1%)**	0/409	(-)	1/380	(-)	1/189	(-)	1/474	(-)
Liver #6	12/8451	(-)	0/309	(-)	0/328	(-)	22/8457	(-)	0/334	(-)
Liver #7	**10/3098**	**(0.3%)**	1/1547	(-)	3/1477	(-)	8/3161	(-)	0/1621	(-)
Liver #8	**13/2442**	**(0.5%)**	1/2378	(-)	6/2312	(-)	1/2564	(-)	1/2507	(-)
Liver #9	**67/13879**	**(0.5%)**	2/5443	(-)	2/5107	(-)	6/13804	(-)	0/5650	(-)
Liver #10	16/7400	(-)	0/3524	(-)	3/3283	(-)	5/7113	(-)	0/3492	(-)
Liver #11	0/412	(-)	1/1328	(-)	**1/295**	**(0.3%)**	0/425	(-)	3/4729	(-)
Liver #12	**4/1098**	**(0.4%)**	1/1389	(-)	0/1272	(-)	2/1102	(-)	0/1544	(-)
Liver #13	**8/2476**	**(0.3%)**	1/2192	(-)	3/2085	(-)	4/2529	(-)	4/5029	(-)
Liver #14	5/3713	(-)	0/2009	(-)	4/1925	(-)	2/3820	(-)	5/3784	(-)
Chronic-NA										
Liver #15	0/339	(-)	0/49	(-)	0/49	(-)	0/338	(-)	0/40	(-)
Liver #16	**28/7278**	**(0.4%)**	0/4403	(-)	6/4053	(-)	14/7556	(-)	6/6084	(-)
Liver #17	**177/945**	**(18.7%)**	0/1059	(-)	0/1009	(-)	0/945	(-)	0/1051	(-)
Liver #18	**13/2655**	**(0.5%)**	0/1239	(-)	0/1185	(-)	**10/2708**	**(0.4%)**	0/1332	(-)
Liver #19	**80/6795**	**(1.2%)**	0/3168	(-)	2/2971	(-)	3/6734	(-)	0/3384	(-)

	M250V/I		A181T/V		N236T		P237H	
Drugs	**ETV**		**ADV**		**ADV**		**ADV**	
Chronic-naive								
Liver #1	**23/2719**	**(0.9%)**	10/3755	(-)	4/4210	(-)	2/4139	(-)
Liver #2	**9/2079**	**(0.4%)**	**2/549**	**(0.4%)**	1/1144	(-)	1/1188	(-)
Liver #3	**10/1699**	**(0.6%)**	**1/298**	**(0.3%)**	3/1636	(-)	1/1666	(-)
Liver #4	**3/388**	**(0.8%)**	**3/549**	**(0.5%)**	0/560	(-)	0/533	(-)
Liver #5	**2/91**	**(2.2%)**	1/409	(-)	0/55	(-)	0/60	(-)
Liver #6	0/214	(-)	**6/305**	**(2.0%)**	**1/294**	**(0.3%)**	0/257	(-)
Liver #7	**7/1289**	**(0.5%)**	4/1531	(-)	**24/2738**	**(0.9%)**	1/2692	(-)
Liver #8	2/1117	(-)	**689/2336**	**(29.5%)**	2/1713	(-)	0/1639	(-)
Liver #9	**27/7325**	**(0.4%)**	**38/5334**	**(0.7%)**	1/6607	(-)	4/6702	(-)
Liver #10	**12/3815**	**(0.3%)**	0/3454	(-)	**13/3245**	**(0.4%)**	2/3272	(-)
Liver #11	**1/199**	**(0.5%)**	1/972	(-)	0/251	(-)	0/251	(-)
Liver #12	**2/672**	**(0.3%)**	**408/1362**	**(30.0%)**	0/598	(-)	0/597	(-)
Liver #13	1/947	(-)	2/2160	(-)	0/1406	(-)	1/1374	(-)
Liver #14	**23/2719**	**(0.9%)**	10/3755	(-)	4/4210	(-)	2/4139	(-)
Chronic-NA								
Liver #15	**1/303**	**(0.3%)**	**2/49**	**(4.1%)**	0/377	(-)	0/384	(-)
Liver #16	1/922	(-)	0/4403	(-)	1/1597	(-)	3/1572	(-)
Liver #17	0/755	(-)	1/1050	(-)	0/698	(-)	**145/698**	**(20.8%)**
Liver #18	1/1464	(-)	2/1206	(-)	0/3156	(-)	0/3107	(-)
Liver #19	8/3834	(-)	**16/3128**	**(0.5%)**	0/3372	(-)	0/3428	(-)

(-): mutant clones less than 0.3% among total clones at each nucleotide sites.
LAM: lamivudine, ADV: adefovir, ETV: entecavir.
doi:10.1371/journal.pone.0035052.t004

Table 5. The prevalence of M204VI mutation at YMDD site in patients before and after entecavir administration.

	Entecavir treatment				
	Before		After		
	Prevalence of the mutated clones		Prevalence of the mutated clones		Period of NA treatment
Serum #3	222/32,238	(0.7%)	2,284/23,791	(9.6%)	2w
Serum #2	401/34,041	(1.2%)	266/25,301	(1.1%)	24w
Serum #5	521/48,723	(1.1%)	245/25,521	(1.0%)	56w
Serum #8	748/65,573	(1.1%)	336/28,702	(1.2%)	48w
Serum #9	312/30,599	(1.0%)	169/14,172	(1.2%)	56w
Serum #1	9/22,843	(-)	2,839/34,162	(8.3%)	8w
Serum #7	26/65,564	(-)	923/66,458	(1.4%)	4w
Serum #12	91/65,616	(-)	258/27,958	(0.9%)	24w
Serum #13	11/23,209	(-)	206/64,747	(0.3%)	32w
Serum #4	3/7,923	(-)	39/65,575	(-)	12w
Serum #6	52/65,582	(-)	77/55,273	(-)	16w
Serum #10	38/22,522	(-)	8/21,053	(-)	8w
Serum #11	47/43,853	(-)	5/16,520	(-)	16w
Serum #14	42/42,784	(-)	40/36,668	(-)	12w

Mutation frequency (%): the ratio of total mutant clones to total aligned coverage at each nucleotide sites.
(-): mutant clones less than 0.3% among total clones at each nucleotide sites.
doi:10.1371/journal.pone.0035052.t005

and the elucidation of other unknown mutations involved in HBe seroconversion are necessary for a better understanding of the underlying mechanisms of HBe seroconversion.

One thing to be noted is that the majority of the chronic-NA cases had extremely low levels of the G1896A pre-C mutant in their liver tissues, even though those cases were serologically positive for anti-HBe and negative for HBeAg. Moreover, entecavir administration significantly reduced the proportion of the G1896A pre-C mutant in the serum of the majority of patients irrespective of their HBeAg serostatus, while the G1896A pre-C mutant clones were detectable in a substantial proportion before treatment in all cases. These findings suggest that the G1896A pre-C mutant have higher sensitivity to NA than the wild-type viruses. Consistent with this hypothesis, several previous studies reported that NA is effective against acute or fulminant hepatitis caused by possible infection with the G1896A pre-C mutant [34,35]. Based on these findings, early administration of NA might be an effective strategy for treating patients with active hepatitis infected predominantly with the G1896A pre-C mutant.

Ultra-deep sequencing has a relatively higher sensitivity than conventional direct population sequencing and is thus useful for detecting drug-resistant mutations not detected by standard sequencing [20,21]. Recently, we revealed that drug-resistant mutants were widely present in treatment-naïve HCV-infected patients, suggesting a putative risk for the expansion of resistant clones to anti-viral therapy [19]. Here, we demonstrated that various drug-resistant HBV variants are present in a proportion of chronically HBV-infected, NA-naïve patients. Several studies using ultra-deep sequencing provided evidence that naturally-occurring drug-resistant mutations are detectable in treatment-naïve individuals with human immunodeficiency virus-1 infection [30,36,37]. Consistent with the cases of human immunodeficiency virus-1 infection, a few studies detected minor variants resistant to NA in the plasma of treatment-naïve patients with chronic HBV infection [20,21]. It remains unclear, however, whether these minor drug-resistant mutations have clinical significance. Our observation of the relative expansion of viral clones with the M204VI mutation during entecavir therapy in some cases indicates the possibility that preexisting minor mutants might provide resistance against NA through the selection of dominant mutant clones. Future studies with a larger cohort size are required to clarify the clinical implications of the latently existing low-abundant drug-resistant mutations.

The current ultra-deep parallel sequencing technology has limitations in the analyses of viral quasispecies. First, because the massively-parallel ultra-deep sequencing platform is based on a multitude of short reads, it is difficult to evaluate the association between nucleotide sites mapped to different genome regions in a single viral clone. Indeed, potential mutational linkages between the pre-C and reverse transcriptase regions were difficult to elucidate due to the short read length of the shotgun sequencing approach. Second, accurate analysis of highly polymorphic viral clones by ultra-deep sequencing is also difficult because the identification of mutations depends strongly on the mapping to the reference genome sequences.

In conclusion, we demonstrated that the majority of patients positive for anti-HBe and negative for HBeAg lacked the predominant infection of the G1896A pre-C mutant in the presence of NA treatment, suggesting that the G1896A pre-C mutant have increased sensitivity to NA therapy compared with wild-type HBV. We also revealed that drug-resistant mutants are widely present, even in the liver of treatment-naïve HBV-infected patients, suggesting that the preexisting low-abundant mutant clones might provide the opportunity to develop drug resistance against NA through the selection of dominant mutations. Further analyses utilizing both novel and conventional sequencing technologies are necessary to understand the significance and clinical relevance of the viral mutations in the pathophysiology of various clinical settings in association with HBV infection.

Supporting Information

Figure S1 Comparison of the viral complexity between the liver and serum of the same individual. Shannon entropy values throughout the whole viral genome of the liver and serum of the representative two cases are shown. (upper two panels, case #11; lower two panels, case #14). preC-C: pre-core~core, preS: pre-surface, P: polymerase.
(TIF)

Table S1 The oligonucleotide primers for amplifying HBV sequences in each clinical specimen.
(DOCX)

Table S2 Error frequency of Ultra-deep sequencing for the expression plasmid encoding wild-type genotype C HBV genome sequences by the three control experiments.
(DOCX)

Table S3 The sensitivity and accuracy of detecting the low abundant minor clones in association with the different coverage numbers.
(DOCX)

Acknowledgments

We thank Prof. G. Tsujimoto, Dr. F. Sato, Dr. Y. Matsumoto, Dr. Y. Endo, Dr. A Takai, Ms. Y. Nakagawa, Ms. K. Fujii and Ms. C. Hirano for ultra-deep sequencing analysis.

Author Contributions

Conceived and designed the experiments: NN HM. Performed the experiments: NN HM. Analyzed the data: NN HM YU AN TF ST KS TC. Contributed reagents/materials/analysis tools: NN HM YU YO TK SY SU. Wrote the paper: NN HM YU KT TC.

References

1. Dienstag JL (2008) Hepatitis B virus infection. N Engl J Med 359: 1486–1500.
2. Lok AS, McMahon BJ (2007) Chronic hepatitis B. Hepatology 45: 507–539.
3. Chang KM (2010) Hepatitis B immunology for clinicians. Clin Liver Dis 14: 409–424.
4. Murray JM, Purcell RH, Wieland SF (2006) The half-life of hepatitis B virions. Hepatology 44: 1117–1121.
5. Ngui SL, Teo CG (1997) Hepatitis B virus genomic heterogeneity: variation between quasispecies may confound molecular epidemiological analyses of transmission incidents. J Viral Hepat 4: 309–315.
6. Hollinger FB (2007) Hepatitis B virus genetic diversity and its impact on diagnostic assays. J Viral Hepat 14 Suppl 1: 11–15.
7. Akahane Y, Yamanaka T, Suzuki H, Sugai Y, Tsuda F, et al. (1990) Chronic active hepatitis with hepatitis B virus DNA and antibody against e antigen in the serum. Disturbed synthesis and secretion of e antigen from hepatocytes due to a point mutation in the precore region. Gastroenterology 99: 1113–1119.
8. Okamoto H, Yotsumoto S, Akahane Y, Yamanaka T, Miyazaki Y, et al. (1990) Hepatitis B viruses with precore region defects prevail in persistently infected hosts along with seroconversion to the antibody against e antigen. J Virol 64: 1298–1303.
9. Kramvis A, Kew MC (1999) The core promoter of hepatitis B virus. J Viral Hepat 6: 415–427.
10. Carman WF, Fagan EA, Hadziyannis S, Karayiannis P, Tassopoulos NC, et al. (1991) Association of a precore genomic variant of hepatitis B virus with fulminant hepatitis. Hepatology 14: 219–222.
11. Omata M, Ehata T, Yokosuka O, Hosoda K, Ohto M (1991) Mutations in the precore region of hepatitis B virus DNA in patients with fulminant and severe hepatitis. N Engl J Med 324: 1699–1704.
12. Domingo E, Gomez J (2007) Quasispecies and its impact on viral hepatitis. Virus Res. Netherlands. pp 131–150.
13. Fishman SL, Branch AD (2009) The quasispecies nature and biological implications of the hepatitis C virus. Infect Genet Evol 9: 1158–1167.
14. Kwon H, Lok AS (2011) Hepatitis B therapy. Nat Rev Gastroenterol Hepatol.
15. Dienstag JL (2009) Benefits and risks of nucleoside analog therapy for hepatitis B. Hepatology 49: S112–121.
16. Ghany MG, Doo EC (2009) Antiviral resistance and hepatitis B therapy. Hepatology 49: S174–184.
17. Zoulim F, Locarnini S (2009) Hepatitis B virus resistance to nucleos(t)ide analogues. Gastroenterology 137: 1593–1608.e1591–1592.
18. Margulies M, Egholm M, Altman WE, Attiya S, Bader JS, et al. (2005) Genome sequencing in microfabricated high-density picolitre reactors. Nature 437: 376–380.
19. Nasu A, Marusawa H, Ueda Y, Nishijima N, Takahashi K, et al. (2011) Genetic heterogeneity of hepatitis C virus in association with antiviral therapy determined by ultra-deep sequencing. PLoS One 6: e24907.
20. Margeridon-Thermet S, Shulman NS, Ahmed A, Shahriar R, Liu T, et al. (2009) Ultra-deep pyrosequencing of hepatitis B virus quasispecies from nucleoside and nucleotide reverse-transcriptase inhibitor (NRTI)-treated patients and NRTI-naive patients. J Infect Dis 199: 1275–1285.
21. Solmone M, Vincenti D, Prosperi MC, Bruselles A, Ippolito G, et al. (2009) Use of massively parallel ultradeep pyrosequencing to characterize the genetic diversity of hepatitis B virus in drug-resistant and drug-naive patients and to detect minor variants in reverse transcriptase and hepatitis B S antigen. J Virol 83: 1718–1726.
22. Han Y, Huang LH, Liu CM, Yang S, Li J, et al. (2009) Characterization of hepatitis B virus reverse transcriptase sequences in Chinese treatment naive patients. J Gastroenterol Hepatol 24: 1417–1423.
23. Ikeda K, Marusawa H, Osaki Y, Nakamura T, Kitajima N, et al. (2007) Antibody to hepatitis B core antigen and risk for hepatitis C-related hepatocellular carcinoma: a prospective study. Ann Intern Med 146: 649–656.
24. Ruike Y, Imanaka Y, Sato F, Shimizu K, Tsujimoto G (2010) Genome-wide analysis of aberrant methylation in human breast cancer cells using methyl-DNA immunoprecipitation combined with high-throughput sequencing. BMC Genomics 11: 137.
25. Louvel S, Battegay M, Vernazza P, Bregenzer T, Klimkait T, et al. (2008) Detection of drug-resistant HIV minorities in clinical specimens and therapy failure. HIV Med 9: 133–141.
26. Ntziora F, Paraskevis D, Haida C, Magiorkinis E, Manesis E, et al. (2009) Quantitative detection of the M204V hepatitis B virus minor variants by amplification refractory mutation system real-time PCR combined with molecular beacon technology. J Clin Microbiol 47: 2544–2550.
27. Matsumoto Y, Marusawa H, Kinoshita K, Endo Y, Kou T, et al. (2007) Helicobacter pylori infection triggers aberrant expression of activation-induced cytidine deaminase in gastric epithelium. Nat Med 13: 470–476.
28. Marusawa H, Matsuzawa S, Welsh K, Zou H, Armstrong R, et al. (2003) HBXIP functions as a cofactor of survivin in apoptosis suppression. EMBO J 22: 2729–2740.
29. Lok AS, Zoulim F, Locarnini S, Bartholomeusz A, Ghany MG, et al. (2007) Antiviral drug-resistant HBV: standardization of nomenclature and assays and recommendations for management. Hepatology 46: 254–265.
30. Hedskog C, Mild M, Jernberg J, Sherwood E, Bratt G, et al. (2010) Dynamics of HIV-1 quasispecies during antiviral treatment dissected using ultra-deep pyrosequencing. PLoS One 5: e11345.
31. Rozera G, Abbate I, Bruselles A, Vlassi C, D'Offizi G, et al. (2009) Massively parallel pyrosequencing highlights minority variants in the HIV-1 env quasispecies deriving from lymphomonocyte sub-populations. Retrovirology 6: 15.
32. Chowdhury A, Santra A, Chakravorty R, Banerji A, Pal S, et al. (2005) Community-based epidemiology of hepatitis B virus infection in West Bengal, India: prevalence of hepatitis B e antigen-negative infection and associated viral variants. J Gastroenterol Hepatol 20: 1712–1720.
33. Orito E, Mizokami M, Sakugawa H, Michitaka K, Ishikawa K, et al. (2001) A case-control study for clinical and molecular biological differences between hepatitis B viruses of genotypes B and C. Japan HBV Genotype Research Group. Hepatology 33: 218–223.
34. Yu JW, Sun LJ, Yan BZ, Kang P, Zhao YH (2011) Lamivudine treatment is associated with improved survival in fulminant hepatitis B. Liver Int 31: 499–506.
35. Lisotti A, Azzaroli F, Buonfiglioli F, Montagnani M, Alessandrelli F, et al. (2008) Lamivudine treatment for severe acute HBV hepatitis. Int J Med Sci 5: 309–312.
36. Simen BB, Simons JF, Hullsiek KH, Novak RM, Macarthur RD, et al. (2009) Low-abundance drug-resistant viral variants in chronically HIV-infected, antiretroviral treatment-naive patients significantly impact treatment outcomes. J Infect Dis 199: 693–701.
37. Lataillade M, Chiarella J, Yang R, Schnittman S, Wirtz V, et al. (2010) Prevalence and clinical significance of HIV drug resistance mutations by ultra-deep sequencing in antiretroviral-naïve subjects in the CASTLE study. PLoS One 5: e10952.

exhibit linear clearance, suggesting that larger individuals clear antibodies more rapidly than smaller individuals without compensatory increases in FcRn-mediated salvage. The effects of other demographic factors, such as age, gender, and renal or hepatic function on the pharmacokinetics of antibodies, are controversial and rarely reported.

An additional clearance mechanism is the development of an immune response against the therapeutic antibody (eg, anti-infliximab or anti-adalimumab antibodies). This affects the pharmacokinetics by increasing clearance, and/or impairing binding. Antiglobulin responses are classed as neutralizing or non-neutralizing, depending on their effect on the activity of the antibody. All therapeutic antibodies approved to date have shown some immunogenicity, even in immunosuppressed patients, although relatively short halve-lives for some chimeric antibodies relative to their FcRn-binding affinity may be related to an enhanced immunogenic response in comparison with human antibodies. On the other hand, the route of administration can sometimes affect immunogenicity, with the intravenous route of administration usually being the least immunogenic. Generally, the intramuscular and subcutaneous routes are more immunogenic. Testing immunogenicity of infliximab and adalimumab in the particular disease of interest is paramount also to understand differential therapeutic effects.

Finally, concomitant administration of other agents that may affect antibody clearance by competing for binding sites, reducing receptor density, or affecting immunogenicity must be considered as potentially affecting clearance. In particular, the role of cotreatment with corticosteroids or immunosuppressive drugs should be further clarified. Beside their impact on therapeutic antibodies immunogenicity, an effect on non-immune-mediated clearance has also been suggested.

Although based on available evidence, the magnitude and the relevance of the correlation between trough levels of anti-TNF therapeutic antibodies and clinical response in inflammatory bowel disease remains unclear, particularly for adalimumab, nonresponders or patients losing response very often have low trough levels. All these considerations point to the urgent need to perform a fine and precise pharmacokinetic profiling, and characterize the pharmacokinetics–pharmacodynamics relationship very early in the development of an antibody therapy, and for any new therapeutic indication. This is key for more successful drug development and to provide greater benefit to patients.

EDOUARD LOUIS
University Hospital CHU of Liège
Liège, Belgium

JULIÁN PANÉS
Hospital Clínic Barcelona
IDIBAPS, CIBERehd
Barcelona, Spain

LARGE-SCALE IDENTIFICATION OF EFFECTOR GENES THAT MEDIATE THE TYPE I INTERFERON ANTIVIRAL RESPONSE

Schoggins JW, Wilson SJ, Panis M, et al. **A diverse range of gene products are effectors of the type I interferon antiviral response. Nature 2011;472:481–485.**

Type I interferons (IFNs) are multifaceted cytokines with a central role in the host innate defense against viral infection. Upon viral infection, the host elicits a type I IFN response, mediated essentially by the expression of hundreds of IFN-stimulated genes (ISGs; Annu Rev Immunol 2005;23:307–336). Although it is assumed that these ISGs function together and are required for establishment of the antiviral state, few have been characterized regarding their antiviral potential, target specificity, and mechanisms of action.

To address these issues, in their recently published paper in the *Nature*, researchers at the Rockefeller University in New York conducted a large-scale, fluorescence-activated, cell sorting-based screen of antiviral ISGs. Based on previously published microarray gene expression data, the authors selected 389 human ISGs as candidate effector genes for screening. Each selected ISG was inserted into a bicistronic lentiviral vector co-expressing the red fluorescent protein TagRFP. The generated lentiviral ISG stocks were used for the transduction of target cells. ISG-TagRFP–expressing target cells were then challenged with a panel of green fluorescent protein-expressing viruses, and viral replication was monitored by quantification of the green fluorescent protein-positive cells in the RFP-positive population. This high-throughput screening strategy allowed for sensitive, quantitative, and systematic evaluation of the antiviral effect of individual ISGs against several medically important viruses, including hepatitis C virus (HCV), HIV, yellow fever virus, West Nile virus, Venezuelan equine encephalitis virus, and chikungunya virus.

Through extensive screening and subsequent validation experiments, they demonstrated that each virus tested was susceptible to inhibition by a unique set of ISGs, with the overall ISG inhibition profile overlapping among viruses. Antiviral ISG hits included broad-acting effectors and specific effectors: The former ISGs including *IRF1, RIG-I, MDA5,* and *IFITM3* showed broad effects on multiple viruses, whereas the latter ISGs, including *DDX60, IFI44L, IFI6,* and *MOV10,* had specific effects on limited viral species. Based on the magnitude of their antiviral effect, the ISGs were categorized as strong inhibitors that broadly act on IFN-mediated or other signaling pathways and modest inhibitors that may have more specific effector functions. Gene ontology analysis classified these validated ISG hits into 3 main molecular functions—nucleic acid binding, hydrolase activity, and helicase activity—and 3 main biologic processes—signal transduction, transcrip-

tion initiation, and small molecule transport. A long-standing hypothesis is that the cooperative action of ISGs is prerequisite for an effective type I IFN response (J Leukoc Biol 2001;69:912–920; Virology 1999;258:435–440). In support of this hypothesis, the authors demonstrated that combinational expression of ISGs generally enhanced their antiviral effects. Surprisingly, they also showed that the expression of several ISGs, including *ADAR, FAM46C, LY6E,* and *MCOLN2,* enhanced viral replication, although how these ISGs do so and why they are induced by IFN signaling remain to be elucidated. Finally, to dissect the antiviral mechanisms of ISGs, they examined the stage of the viral life cycle at which the validated ISGs exert their antiviral functions. The assays using HCV pseudoparticles and subgenomic replicons expressing reporter gene revealed that translational block is the primary and common antiviral mechanism of these effector ISGs, highlighting the surprising host strategy that multiple effectors with diverse molecular functions cooperatively suppress HCV by targeting a single HCV life-cycle stage.

Together, the identification and characterization of novel antiviral effectors presented in this study unraveled the heretofore unsuspected diversity of ISG-mediated IFN effector mechanisms.

Comments. The innate immune response represents the first line of defense against viral assault. Type I IFNs, a family of cytokines with pleiotropic functions, are central players in antiviral innate immunity (Annu Rev Immunol 2005;23:307–336). Since the first description of IFN as a soluble factor produced by influenza virus-infected chick embryo cells that confers resistance to subsequent virus infection (Proc R Soc Lond B 1957;147:258–267), several outstanding studies have contributed to our understanding of many important aspects of IFN system (Immunity 2006;25:343–348). Notably, there is now substantial knowledge about the virus-sensing machineries that lead to type I IFN induction and IFN receptors and their downstream pathway, the so-called JAK–Stat signaling pathway (Nat Immunol 2006;7:131–137; Immunity 2006; 25:361–372).

Activation of the JAK–Stat pathway through IFN receptors induces the expression of numerous ISGs. Most of the well-characterized examples of ISGs are 2′-5′ oligoadenylate synthases, double-stranded RNA-dependent protein kinase R (PKR), and myxovirus resistance proteins. The 2′-5′ oligoadenylate synthases, activated by viral dsRNA, produce 2′-5′ oligoadenylates, which in turn activate the latent nuclease RNase L, resulting in the degradation of viral RNA transcripts as well as host RNAs (Annu Rev Biochem 1998;67:227–264). PKR, a member of the eukaryotic initiation factor 2α kinase family, is another ISG. Activation of PKR by dsRNA results in eukaryotic initiation factor 2α phosphorylation, leading to the translational block of viral and cellular mRNA (Cell 1990; 62:379–390). Myxovirus resistance proteins, large IFN-inducible GTPases of the dynamin family, have antiviral activity against influenza and vesicular stomatitis virus (Cell 1990;62:51–61; Ciba Found Symp 1993;176:233–243). Their similarity with dynamin suggests that they interfere with viral assembly and trafficking in the cell. Furthermore, in association with HCV, ISG56 was recently demonstrated to suppress HCV RNA translation through direct interaction with eIF3, which blocks ribosome recruitment to the viral RNA (J Virol 2004;78: 11591–11604).

Although these examples clearly suggest that ISGs represent essential effector components of IFN signaling to establish an "antiviral state" and indeed hundreds of ISGs have been identified since their discovery >25 years ago (Proc Natl Acad Sci U S A 1979;76:1824–1828; Proc Natl Acad Sci U S A 1984;81:6733–6737; J Leukoc Biol 2001; 69:912–920), the majority of ISGs remain to be characterized with respect to their antiviral activity. Thus, "antiviral state" is a generic term and the larger picture of how the IFN system exerts an antiviral response through the induction of numerous ISGs has long been an open question for most researchers in this field.

These novel findings presented by Schoggins et al provide a long-sought answer for this challenging theme. Overcoming the technical barriers that hampered the systematic overexpression of hundreds of genes, they developed an elegant, cell-based screening system by which they identified multiple novel antiviral ISGs. The major findings of this study are as follows. Each ISG has a diverse range of antiviral potential and virus target specificity. ISGs exert their antiviral effect in a combinatorial fashion, and translational inhibition is a common mechanism of ISG-mediated antiviral action. These findings, together with the fact that IFN therapy is currently the first-choice therapy for HCV eradication and is also used for the treatment of several other viral infections, have potentially important implications for the development of new antiviral therapies. The side effects of IFN therapy, which frequently limit its clinical use, may be due to undesirable global ISG expression. Thus, selective utilization of ISG sets optimized for target viruses might be a more effective and safer therapeutic option.

This work is very exciting and expands our knowledge of downstream IFN effector mechanisms. However, some issues remain to be resolved in future studies. First, the effects of viral evasion mechanisms are dismissed in this study. Most viruses have evolved unique strategies to interfere with various aspects of the IFN system (Nat Rev Immunol 2002;2:675–687). For example, HCV is equipped with multiple evasion mechanisms: NS3/4A serine protease blockade of type I IFN production by the cleavage of IPS-1, a key signaling molecule of the IFN-inducing pathway (Trends Immunol 2006;27:1–4), disruption of JAK–Stat signaling by NS5A, and inhibition of PKR by NS5A and E2 proteins (Nat Rev Immunol 2002;2:675–687). The overexpression platform used in this study may not reflect the events that actually happen during viral infection in vivo. Second, further investigation of the proviral ISGs presented in this study is needed. It is of great interest that several ISGs exhibit proviral activity and the data suggest

that the effect of IFN is more complex than previously thought. What are the physiologic functions of proviral ISGs and why does the IFN system induce them? A loss-of-function study might be useful to answer these questions. Finally, the screening assays were performed on only positive-sense RNA viruses (HCV, yellow fever virus, Venezuelan equine encephalitis virus, West Nile virus, and chikungunya virus) and 1 retrovirus (HIV-1), but not on DNA viruses. Yet the host also obviously activates the type I IFN system against DNA viruses, such as cytomegalovirus and herpes simplex virus, utilizing Toll-like receptor 9 and a not-yet identified cytoplasmic DNA sensor molecule(s) (Nat Immunol 2006;7:131-137; Curr Opin Immunol 2010;22:41-47; Biochem Pharmacol 2010;80:1955-1972). Given that DNA viruses have their own viral life cycle and evasion strategies distinct from those of viruses tested here, there might be other antiviral ISG profiles with mechanisms of action that are entirely unique to DNA viruses. Elucidation of these issues, together with further dissection of the antiviral mechanisms of the validated ISGs, would provide additional insight into the type I IFN antiviral response.

In conclusion, this is the first report of a comprehensive evaluation of antiviral potentials of ISGs. A newly developed, cell-based screening assay identified multiple novel antiviral effectors in the type I IFN system that were previously unanalyzable. Given that current IFN therapy has undesirable side effects, this work opens the door to designing new therapeutic strategies based on antiviral ISGs.

KEN TAKAHASHI
HIROYUKI MARUSAWA
TSUTOMU CHIBA
Department of Gastroenterology and Hepatology
Graduate School of Medicine, Kyoto University
Kyoto, Japan

DIAGNOSTIC ENDOSCOPIC RETROGRADE PANCREATOGRAPHY FOR AUTOIMMUNE PANCREATITIS: ONE SIZE DOES NOT FIT ALL

Sugumar A, Levy MJ, Kamisawa T, et al. **Endoscopic retrograde pancreatography criteria to diagnose autoimmune pancreatitis: an international multicentre study. Gut 2011;60:666-670.**

Autoimmune pancreatitis (AIP) is being increasingly recognized worldwide. Although the exact etiology and pathogenesis of AIP remain unclear, we do have some insights into the disease process. It has been proposed that AIP is the pancreatic manifestation of an immunoglobulin (Ig)G4-associated systemic fibro-inflammatory disorder that can also affect the bile duct, kidneys, retroperitoneum, orbits, lymph nodes, and salivary glands (Pancreatology 2006;6:132-137). Histologically, AIP is characterized by an inflammatory process, with infiltration of the pancreas by a lymphoplasmactic infiltrate rich in IgG4-positive cells. The inflammatory process can be focal or diffuse. Additionally, IgG4-positive plasma cells and other inflammatory cells have been described as infiltrating other organs in patients with AIP (J Gastroenterol 2003;38:982-984), thus supporting the notion that this process may be systemic. Clinically, AIP presents most commonly as obstructive jaundice; this presentation can often be confused with pancreatic adenocarcinoma. Less commonly, AIP can present with abdominal pain or acute pancreatitis. AIP is treated with a course of corticosteroids, and the response to treatment is often dramatic. A reliable and accurate diagnosis of the disease, particularly differentiation from pancreatic adenocarcinoma, which AIP can mimic, continues to present a clinical challenge (Clin Gastroenterol Hepatol 2006;4:1010-1016; Am J Gastroenterol 2003;98:2694-2699). Histology, considered to be the gold standard for diagnosis, requires a biopsy that is often not easily obtainable in the pancreas. Fine-needle aspiration of the pancreas, although readily available, does not yield a definitive diagnosis of AIP (Clin Gastroenterol Hepatol 2006;4:1010-1016). A core biopsy may be diagnostic, with the caveat that, with patchy distribution of disease or in the presence of a strong desmoplastic reaction, even a core specimen may not yield a diagnosis. Thus, in the appropriate clinical setting, a negative biopsy does not exclude pancreatic cancer or AIP. A surgical biopsy, although certainly not feasible in all cases, may thus be required for diagnosis. Investigators in Asia and the United States have developed several diagnostic classification systems based on clinical, imaging, laboratory, and pathologic criteria, and response to treatment. According to the Japanese Pancreas Society, a diagnosis of AIP can be made when a patient exhibits ≥ 1 imaging feature and either 1 serologic or histologic feature. The Mayo HISORt criteria are more commonly used in the United States, and include ≥ 1 of the following: diagnostic histology, characteristic imaging, elevated serum IgG4 levels, involvement of other organ systems, and response to treatment with glucocorticoids. Although there seems to be an emerging consensus toward uniformity in the criteria, some major differences remain, 1 of which is the use of endoscopic retrograde cholangiopancreatography (ERCP)for ductal imaging; the Asian criteria mandate endoscopic retrograde pancreatography (ERP) for ductal imaging (J Gastroenterol 2006;41:626-631), whereas the Mayo HISORt criteria do not (J Gastroenterol 2007;42[Suppl 18]:39-41).

To advance our understanding of AIP, an international group of experts has formed the Autoimmune Pancreatitis International Cooperative Study group. Given the discrepancy in the use of ERP to diagnose AIP, 1 of the first goals of this collaboration was to determine the performance characteristics of ERP for the diagnosis of AIP.

Sugumar et al performed an international, multicenter study in 2 phases (Gut 2011;60:666-670). A total of 21 physicians from 4 centers in Asia, the United Kingdom,

PLOS ONE

A Subclone of HuH-7 with Enhanced Intracellular Hepatitis C Virus Production and Evasion of Virus Related-Cell Cycle Arrest

Asako Murayama[1], Nao Sugiyama[1], Seiko Yoshimura[2], Mitsuko Ishihara-Sugano[2], Takahiro Masaki[1], Sulyi Kim[1], Takaji Wakita[1], Shunji Mishiro[3], Takanobu Kato[1]*

1 Department of Virology II, National Institute of Infectious Diseases, Tokyo, Japan, **2** Corporate Research and Development Center, Toshiba Corporation, Kanagawa, Japan, **3** Department of Medical Sciences, Toshiba General Hospital, Tokyo, Japan

Abstract

Hepatitis C virus (HCV) cell culture system with JFH-1 strain and HuH-7 cells enabled us to produce infectious HCV particles *in vitro*, and such system is useful to explore the anti-HCV compounds and to develop the vaccine against HCV. In the present study, we describe the derivation of a cell line that permits improved production of HCV particles. Specifically, we characterized several subclones that were isolated from the original HuH-7 cell line by limiting dilution. These HuH-7 subclones displayed a notable range of HCV production levels following transfection by full-genome JFH-1 RNA. Among these subclones, HuH-7T1 produced HCV more efficiently than other subclones and Huh-7.5.1 that is known to be highly permissive for HCV replication. Upon transfection with full-genome RNA, HCV production was increased ten-fold in HuH-7T1 compared to Huh-7.5.1. This increase in viral production correlated with increased efficiency of intracellular infectious virus production. Furthermore, HCV replication did not induce cell cycle arrest in HuH-7T1, whereas it did in Huh-7.5.1. Consequently, the use of HuH-7T1 as host cells could provide increased population of HCV-positive cells and elevated viral titer. In conclusion, we isolated a HuH-7 subclone, HuH-7T1, that supports efficient HCV production. High efficiency of intracellular infectious virus production and evasion of cell cycle arrest were important for this phenotype. We expect that the use of this cell line will facilitate analysis of the underlying mechanisms for HCV particle assembly and the cell cycle arrest caused by HCV.

Citation: Murayama A, Sugiyama N, Yoshimura S, Ishihara-Sugano M, Masaki T, et al. (2012) A Subclone of HuH-7 with Enhanced Intracellular Hepatitis C Virus Production and Evasion of Virus Related-Cell Cycle Arrest. PLoS ONE 7(12): e52697. doi:10.1371/journal.pone.0052697

Editor: Kui Li, University of Tennessee Health Science Center, United States of America

Received July 25, 2012; **Accepted** November 19, 2012; **Published** December 20, 2012

Funding: This work was supported in part by Grants-in-Aid for Scientific Research from the Japan Society for the Promotion of Science, from the Ministry of Health, Labour and Welfare of Japan, and from the Ministry of Education, Culture, Sports, Science and Technology. The funders had no role in study design, data collection and analysis, decision to publish, or preparation of the manuscript.

Competing Interests: SY, MIS and SM are employees of Toshiba Corporation. There are no patents, products in development or marketed products to declare. This does not alter the authors' adherence to all the PLOS ONE policies on sharing data and materials, as detailed online in the guide for authors.

* E-mail: takato@nih.go.jp

Introduction

Hepatitis C virus (HCV) is a major cause of chronic liver disease [1,2]. Currently, approximately 200 million people are infected with HCV worldwide and are at continued risk of developing chronic liver diseases such as chronic hepatitis, liver cirrhosis, and hepatocellular carcinoma [3,4]. Historically, the lack of a cell culture system capable of producing virus particles hampered progress in the field of HCV research. Subsequently, a robust HCV cell culture system was developed using HCV JFH-1 strain that had been cloned from a fulminant hepatitis patient [5,6,7]. JFH-1 was the first HCV strain that could replicate and produce HCV particles autonomously *in vitro*, thereby facilitating investigation of the entire life cycle of the virus. This HCV cell culture system employed HuH-7 cell line, which was established from a hepatocellular carcinoma [5,8], as a host. Since the HCV replicon system enabling HCV subgenomic RNA replication was originally developed using HuH-7 [9], this cell line has been used in the research field of HCV most frequently. However, HuH-7 is known to be heterogeneous. Notably, Saintz et al. reported that HuH-7 cell lines obtained from various laboratories exhibit distinct morphological, cell growth, and HCV susceptibility properties [10]. We also found that single-cell cloning of HuH-7 maintained in our laboratory yielded multiple subclones that exhibited different characteristics of HCV infection and replication [11]. In the present study, we derived cell lines from original HuH-7 obtained from the cell bank and screened to identify a cell line with improved production of infectious HCV particles. As we report here, we obtained one such clone (HuH-7T1) and performed an initial characterization of the HCV life cycle in this host.

Materials and Methods

Cell culture

The original HuH-7 cell line (catalog number; JCRB0403) was purchased from Health Science Research Resources Bank (Osaka, Japan). The cured cell line, Huh-7.5.1, was a kind gift from Dr. Francis V. Chisari (Scripps Research Institute, La Jolla, CA) [6]. These cell lines were cultured at 37°C in a 5% CO_2 environment using Dulbecco's Modified Eagle's Medium containing 10% fetal bovine serum.

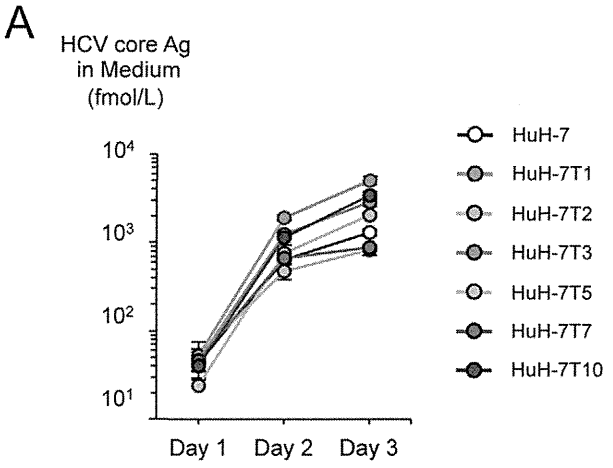
A
HCV core Ag
in Medium
(fmol/L)
10^4
10^3
10^2
10^1
Day 1
Day 2
Day 3
HuH-7
HuH-7T1
HuH-7T2
HuH-7T3
HuH-7T5
HuH-7T7
HuH-7T10

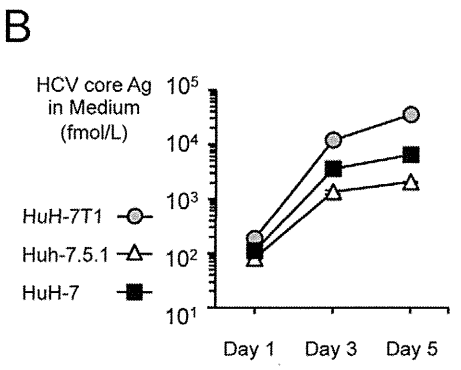
B
HCV core Ag
in Medium
(fmol/L)
10^5
10^4
10^3
10^2
10^1
HuH-7T1
Huh-7.5.1
HuH-7
Day 1
Day 3
Day 5

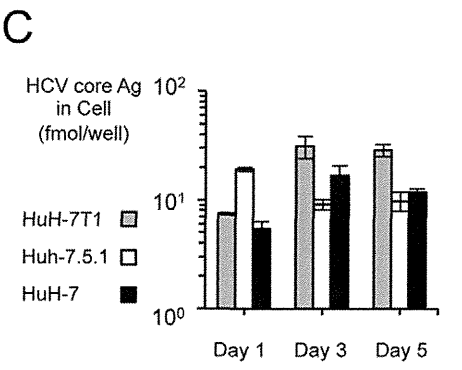
C
HCV core Ag
in Cell
(fmol/well)
10^2
10^1
10^0
HuH-7T1
Huh-7.5.1
HuH-7
Day 1
Day 3
Day 5

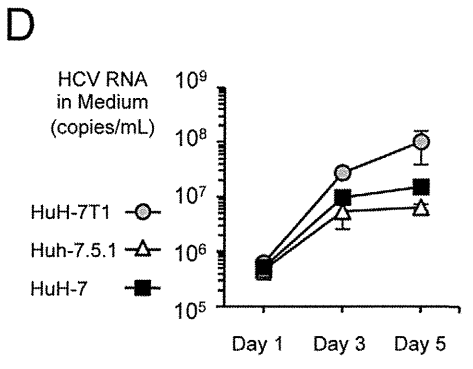
D
HCV RNA
in Medium
(copies/mL)
10^9
10^8
10^7
10^6
10^5
HuH-7T1
Huh-7.5.1
HuH-7
Day 1
Day 3
Day 5

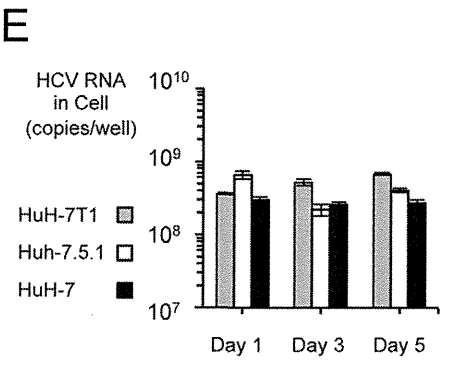
E
HCV RNA
in Cell
(copies/well)
10^{10}
10^9
10^8
10^7
HuH-7T1
Huh-7.5.1
HuH-7
Day 1
Day 3
Day 5

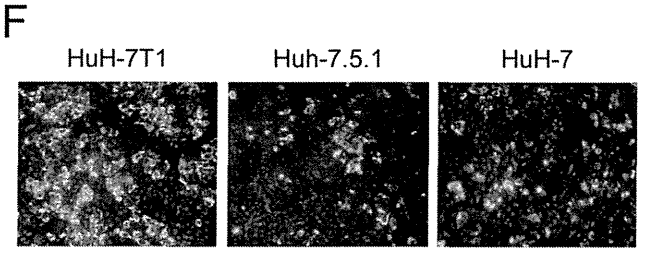
F
HuH-7T1
Huh-7.5.1
HuH-7

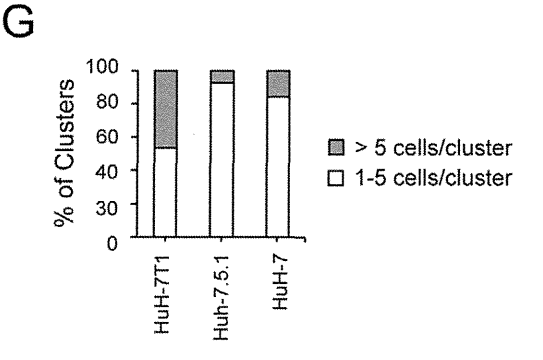
G
% of Clusters
100
80
60
40
30
0
HuH-7T1
Huh-7.5.1
HuH-7
> 5 cells/cluster
1-5 cells/cluster

Figure 1. HCV production in HuH-7 subclones. (A) Two micrograms of JFH-1 RNA were electroporated into the HuH-7 subclones. Culture medium was harvested at Days 1, 3, and 5, and HCV core protein levels in the culture medium were measured. Assays were performed three times independently, and data are presented as mean ± standard deviation. (B–D) Comparison of HCV production among HuH-7T1, Huh-7.5.1 and HuH-7. HCV core protein (B and C) and HCV RNA (D and E) levels in cells and culture medium were measured. Assays were performed three times independently, and data are presented as mean ± standard deviation. (F) HCV-positive cells at Day 3 post-transfection were visualized with anti-core antibody (green); nuclei were visualized with DAPI (blue). (G) The number of HCV positive cells within a cluster were counted and classified into 2 groups (>5 cells/cluster and 1–5/cluster). More than 100 foci were counted. The percentages of each group are shown.
doi:10.1371/journal.pone.0052697.g001

Single cell cloning by limiting dilution

The original HuH-7 cell line was diluted with medium at 1 cell/mL and seeded at 100 μL/well in 96-well plates. Six subclones were obtained and resulting subclones were expanded and stored at −80°C pending further characterization. The characteristics of obtained subclones were maintained after passages over several months.

HCV constructs and RNA transfection

pJFH1 is a full-length JFH-1 clone whose construction was reported previously [5]. pSGR-JFH1-Luc (a JFH-1 subgenomic replicon construct containing a firefly luciferase-encoding reporter gene) and pSGR-JFH1/GND-Luc (a replication-defective mutant construct) also were described previously [12]. pH77S.2, a full-length H77S.2 construct, was a kind gift from Dr. Stanley M Lemon (University of North Carolina at Chapel Hill, Chapel Hill, NC). This construct is a derivative of strain H77S (genotype 1a) harboring an additional mutation, and produces infectious virus in cultured cells after full-genome RNA transfection [13]. RNA synthesis and transfection were performed as described previously [14,15].

Quantification of HCV core protein and RNA

The concentration of HCV core protein in the culture medium and cell lysate was measured using a chemiluminescent enzyme immunoassay (Lumipulse Ortho HCV antigen, Fujirebio, Tokyo, Japan) in accordance with the manufacturer's instructions. The concentration of HCV RNA was measured as described previously [16].

Determination of infectivity titers

To determine the intracellular infectivity of the HCV RNA-transfected cells, a cell lysate of HCV RNA-transfected cells cultured in a 10 cm dish was generated by subjecting the cells to four freeze-thaw cycles. The culture supernatant and cell lysate were serially diluted and inoculated into naive Huh-7.5.1 seeded at 1×10^4 cells/well in poly-D-lysine-coated 96-well plates (BD, Franklin Lakes, NJ), and the inoculated plates were incubated for another 3 days at 37°C. The cells were then fixed with methanol, and the infected foci were visualized by staining with anti-core antibody (clone 2H9 [5,8] for JFH-1 and c7-50 (Abcam, Cambridge, MA) for H77S.2) and Alexa Fluor 488 Goat Anti-mouse IgG (Invitrogen, Carlsbad, CA). The infectivity titer was quantified by counting the stained foci and expressing the value as the number of focus-forming units (FFU).

Table 1. Infectivity titers in culture medium and cells of HuH-7T1 and Huh-7.5.1 transfected with JFH-1 RNA.

Cell Line	Infectivity		Secretion Rate
	Medium (FFU/dish)	Cells (FFU/dish)	
HuH-7T1	$2.23\times10^6\pm3.15\times10^5$ *	$1.11\times10^4\pm1.15\times10^3$ *	$2.00\times10^2\pm1.98\times10^1$ *
Huh-7.5.1	$9.92\times10^4\pm2.98\times10^4$	$1.34\times10^2\pm1.42\times10^1$	$7.30\times10^2\pm1.40\times10^2$

*$P<0.05$ as compared with Huh-7.5.1.
doi:10.1371/journal.pone.0052697.t001

Flow cytometric analysis

For cell cycle distribution analyses, cells were labeled with 5-ethynyl-2′-deoxyuridine (EdU) for 4 h prior to harvest. The harvested cells were fixed in 4% paraformaldehyde, permeabilized, and stained with anti-nonstructural (NS) 5A antibody (clone KS0265-1; raised by immunization with JFH-1 NS5A) and Alexa Fluor 647 Goat Anti-mouse IgG (Invitrogen). Incorporated EdU was stained with Alexa Fluor 488 azide by using the Click-iT EdU flow cytometry kit (Invitrogen) according to the manufacturer's instructions. Following treatment with RNase A, 7-aminoactinomycin D (7-AAD) was added. Samples were analyzed using a FACS Calibur flow cytometer. The population of cells in G0/G1, S, or G2/M phases of the cell cycle was determined using FlowJo software (Tree Star, Inc., Ashland, OR).

Immunostaining

Infected cells were cultured on glass cover slips in a 12-well plate. Cells were fixed in 4% paraformaldehyde and permeabilized. After blocking, HCV-positive cells were visualized by staining with anti-core antibody (clone 2H9) and Alexa Fluor 488 Goat Anti-mouse IgG, and nuclei were stained with 4′, 6-diamidino-2-phenylindole (DAPI).

Virus entry assay

HCV pseudo type virus (HCVpp) harboring the JFH-1 E1 and E2 glycoprotein was prepared as described previously [11]. Target

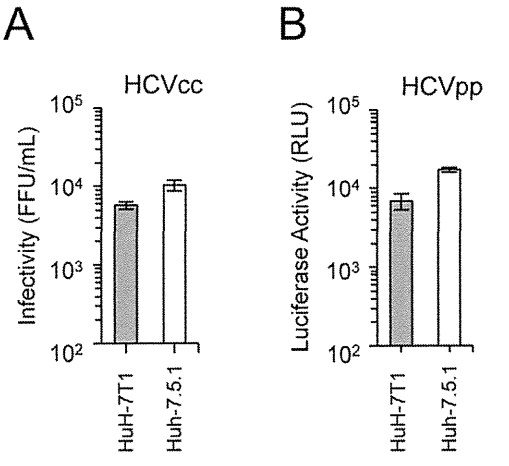

Figure 2. Comparison of infection in HuH-7T1 and Huh-7.5.1. (A) Infection of HCVcc into HuH-7T1 and Huh-7.5.1. The cells were fixed 3 days after infection and infected foci were counted. (B) Infection of HCVpp into HuH-7T1 and Huh-7.5.1. The cells were harvested 3 days after infection, and the luciferase activity in the cell lysate was measured.
doi:10.1371/journal.pone.0052697.g002

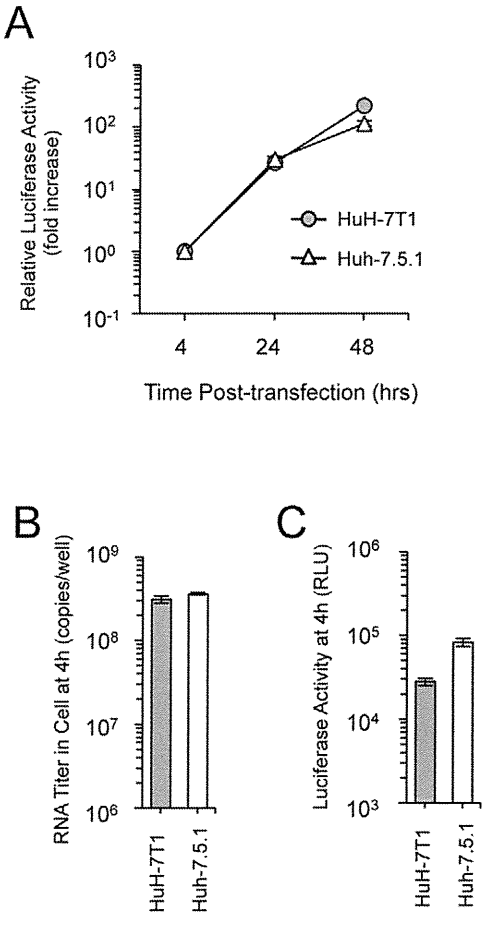

Figure 3. Comparison of replication in HuH-7T1 and Huh-7.5.1. (A) Five micrograms of JFH-1 subgenomic replicon RNA was electroporated into HuH-7T1 and Huh-7.5.1. The cells were harvested at indicated time points. The luciferase activity in the cell lysates was normalized to the data at 4 h after transfection; values are expressed as fold increases. (B and C) Comparison of transfection and translation efficiencies. Five micrograms of JFH-1/GND-Luc RNA was transfected into HuH-7T1 and Huh-7.5.1. The cells were harvested at 4 h after transfection, and the amount of transfected RNA in cells (B) and luciferase activity in the cell lysates (C) were measured.
doi:10.1371/journal.pone.0052697.g003

cells were seeded into 48-well plates at a density of 2×10^4 cells/well. On the following day, a 100-μL aliquot of each diluted supernatant containing HCVpp was added to each well and incubated for 3 h. The supernatants were replaced with fresh medium, and the cells were incubated for 72 h at 37°C. Cells were lysed with Passive Lysis Buffer (Promega, Madison, WI). Luciferase activities were quantified using a luciferase assay system (Promega). Assays were performed in triplicate; data are presented as mean ± standard deviation.

Cell culture-generated HCV JFH-1 virus (HCVcc) was prepared as follows: culture medium from JFH-1 RNA-transfected cells was collected and 40-times concentrated using Amicon Ultra-15 filter units (100-kDa cutoff; Millipore, Bedford, MA) and stored at −80°C until use. HCVcc was inoculated into target cells, and infectivity titer was determined as described.

Luciferase assay

Luciferase activity of subgenomic reporter replicon RNA-transfected cell lysate was measured as described previously [14,15].

Statistical analysis

Significant differences were evaluated using the Student's t-test. $P<0.05$ was considered significant.

Results

Isolation of HuH-7 subclones with improved HCV production

To obtain cell lines with improved HCV production potential, we used limiting dilution to establish six subclones (HuH-7T1, HuH-7T2, HuH-7T3, HuH-7T5, HuH-7T7, and HuH-7T10) from the original HuH-7 purchased from the cell bank. We transfected JFH-1 RNA into each of these subclones and measured the level of core protein in the culture medium. These subclones displayed a range of core protein production levels. (Fig. 1A). Compared to the original HuH-7, four (HuH-7T1, HuH-7T3, HuH-7T5 and HuH-7T10) and two (HuH-7T2 and HuH-7T7) subclones produced higher or lower amounts of HCV core protein, respectively. Among these subclones, we chose HuH-7T1 for further characterization because this subclone produced HCV core protein at the highest level (Fig. 1A). Then, we compared core protein production of HuH-7T1 with Huh-7.5.1, a cell line reported to be highly permissive for HCV replication [6]. After JFH-1 RNA transfection, HCV core protein level in the culture medium of HuH-7T1 was 17.6-fold higher than that seen with Huh-7.5.1 (Fig. 1B). HCV core protein levels in cell lysate of HuH-7T1 were lower at Day 1, but higher at Days 3 and 5 after transfection, compared to Huh-7.5.1 (Fig. 1C). HCV RNA levels in the culture medium and cell lysates of these cells showed similar tendencies (Fig. 1D and 1E). The infectivity titer in culture medium of HuH-7T1 at Day 5 was 22.5-fold higher than that of Huh-7.5.1 (Table 1), indicating that HuH-7T1 supported production of infectious HCV particles to levels higher than those seen in Huh-7.5.1. The number of HCV-positive cells of HuH-7T1 at Day 5 also was higher than that seen with Huh-7.5.1 (Fig. 1F). The percentage of HCV positive cell clusters consisting of more than 5 cells was higher in HuH-7T1 than in Huh-7.5.1 (Fig. 1G). We also assessed if HuH-7T1 produced higher amount of core protein after infection of HCVcc. HuH-7T1 produced higher amount of HCV core protein than Huh-7.5.1 after JFH-1 virus infection at the same multiplicity of infection (Fig. S1A), and HCV core protein levels in cell lysate of HuH-7T1 were also higher than that of Huh-7.5.1 (Fig. S1B). These data indicated that HuH-7T1 produced infectious HCV particles more efficiently than Huh-7.5.1 after JFH-1 RNA transfection and JFH-1 virus infection.

The original HuH-7 could produce higher amount of HCV core protein than Huh-7.5.1 after JFH-1 RNA transfection (Fig. 1B). However, in the experiment of HCVcc infection, HuH-7 produced lower amount of HCV core protein than Huh-7.5.1 in culture medium (Fig. S1A) and in cell lysate (Fig. S1B).

Analysis of HCV life cycle in HuH-7T1

To clarify the underlying mechanism of the enhanced virus production in HuH-7T1, we assessed the efficiencies of each step in the HCV life cycle. The viral infection step was assessed by using HCVcc and HCVpp. The HCVcc system uses cell culture-generated HCV and detects steps from viral attachment through replication. On the other hand, the HCVpp system uses the